Journal of Geophysical Research: Atmospheres

RESEARCH ARTICLE
10.1029/2018JD028491

Regional Similarities and NO_x-Related Increases in Biogenic Secondary Organic Aerosol in Summertime Southeastern United States

Jun Liu[1,2], Lynn M. Russell[1], Giulia Ruggeri[3], Satoshi Takahama[3], Megan S. Claflin[4], Paul J. Ziemann[4], Havala O. T. Pye[5], Benjamin N. Murphy[5], Lu Xu[6], Nga L. Ng[7,8], Karena A. McKinney[9], Sri Hapsari Budisulistiorini[10], Timothy H. Bertram[11], Athanasios Nenes[7], and Jason D. Surratt[12]

[1]Scripps Institution of Oceanography, University of California, San Diego, La Jolla, CA, USA, [2]Now at Department of Chemistry, University of Michigan, Ann Arbor, MI, USA, [3]ENAC/IIE Swiss Federal Institute of Technology Lausanne (EPFL), Lausanne, Switzerland, [4]Department of Chemistry and Biochemistry and Cooperative Institute for Research in Environmental Sciences, University of Colorado Boulder, Boulder, CO, USA, [5]National Exposure Research Laboratory, U.S. Environmental Protection Agency, Research Triangle Park, NC, USA, [6]Division of Geological and Planetary Sciences, California Institute of Technology, Pasadena, CA, USA, [7]School of Chemical and Biomolecular Engineering, Georgia Institute of Technology, Atlanta, GA, USA, [8]School of Earth and Atmospheric Sciences, Georgia Institute of Technology, Atlanta, GA, USA, [9]School of Engineering and Applied Sciences, Harvard University, Cambridge, MA, USA, [10]Earth Observatory of Singapore, Nanyang Technological University, Singapore, [11]Department of Chemistry, University of Wisconsin-Madison, Madison, WI, USA, [12]Department of Environmental Sciences and Engineering, Gillings School of Global Public Health, University of North Carolina at Chapel Hill, Chapel Hill, NC, USA

Key Points:
- Aerosol concentration and composition are largely similar at two different forested sites during summertime in the southeastern United States
- FTIR of ambient biogenic SOA factors are similar to isoprene and monoterpene chamber experiment, supporting NO_x-related oxidation pathways
- NO_x increases biogenic SOA by 0.5 ± 0.1 μg/m^3 for CTR-LO-OOA and 1.0 ± 0.3 μg/m^3 for CTR-BOA for each ppb NO_x above 1 ppb at Centreville but not at Look Rock (where NO_x was usually below 1 ppb)

Supporting Information:
- Supporting Information S1

Correspondence to:
L. M. Russell,
lmrussell@ucsd.edu

Citation:
Liu, J., Russell, L. M., Ruggeri, G., Takahama, S., Claflin, M. S., Ziemann, P. J., et al. (2018). Regional similarities and NO_x-related increases in biogenic secondary organic aerosol in summertime southeastern United States. *Journal of Geophysical Research: Atmospheres*, *123*, 10,620–10,636. https://doi.org/10.1029/2018JD028491

Received 7 FEB 2018
Accepted 24 JUL 2018
Accepted article online 4 AUG 2018
Published online 17 SEP 2018

Abstract During the 2013 Southern Oxidant and Aerosol Study, Fourier transform infrared spectroscopy (FTIR) and aerosol mass spectrometer (AMS) measurements of submicron mass were collected at Look Rock (LRK), Tennessee, and Centreville (CTR), Alabama. Carbon monoxide and submicron sulfate and organic mass concentrations were 15–60% higher at CTR than at LRK, but their time series had moderate correlations ($r \sim 0.5$). However, NO_x had no correlation ($r = 0.08$) between the two sites with nighttime-to-early-morning peaks 3–10 times higher at CTR than at LRK. Organic mass (OM) sources identified by FTIR Positive Matrix Factorization (PMF) had three very similar factors at both sites: fossil fuel combustion-related organic aerosols, mixed organic aerosols, and biogenic organic aerosols (BOA). The BOA spectrum from FTIR is similar (cosine similarity > 0.6) to that of lab-generated particle mass from the photochemical oxidation of both isoprene and monoterpenes under high NO_x conditions from chamber experiments. The BOA mass fraction was highest during the night at CTR but in the afternoon at LRK. AMS PMF resulted in two similar pairs of factors at both sites and a third nighttime NO_x-related factor (33% of OM) at CTR but a daytime nitrate-related factor (28% of OM) at LRK. NO_x was correlated with BOA and LO-OOA for NO_x concentrations higher than 1 ppb at both sites, producing 0.5 ± 0.1 μg/m^3 for CTR-LO-OOA and 1.0 ± 0.3 μg/m^3 for CTR-BOA additional biogenic OM for each 1 ppb increase of NO_x.

1. Introduction

Biogenic secondary organic aerosols (SOAs) are estimated to be increased by as much as 78% because of interactions involving anthropogenic emissions on the U.S. east coast (Carlton et al., 2010) and in eastern Asia (Matsui et al., 2014). The resulting aerosol particle mass may account for as much as 70% of the global organic aerosol budget (Spracklen et al., 2011). More than 90% of sulfate (from SO_2) and nitrogen oxides (NO_x, or NO + NO_2) are anthropogenic and increase the yield of biogenic SOAs (Shilling et al., 2013; Shrivastava et al., 2017; Spracklen et al., 2011; Xu et al., 2015). For example, some field studies have shown that a 1 μg/m^3 decrease in sulfate can lead to a 0.2–0.42 μg/m^3 decrease in isoprene SOA (Blanchard et al., 2016; Budisulistiorini et al., 2017; Pye et al., 2013; Shrivastava et al., 2017; Xu et al., 2015, 2016). Similarly, decreases in NO_x have been shown to decrease biogenic SOA formation but there are also studies that have shown increases of biogenic SOA in some regimes with decreased NO_x (Table 1; de Sa et al., 2017; Edwards et al., 2017; Kroll et al., 2006; Lane et al., 2008; Liu et al., 2016; Matsui et al., 2014; Ng et al., 2007; Pye et al., 2010, 2013, 2015; Rollins et al., 2012; Wildt et al., 2014; Xu et al., 2014, 2015; Zhang et al., 2017; Zheng et al., 2015). Since these effects of NO_x have been shown by laboratory studies to affect biogenic SOA formation by

Table 1
Summary of Effects of NO_x on Biogenic SOA Formation From Field Studies and Model Simulations

Simulated effect	Effect of NO_x on bSOA	Model version	Mechanism	Reference
25% of NO_x reduction will increase 5% bSOA from June to August 2006 in Southeastern United States.	Negative	CMAQ5.0	SOA formation based on semivolatile organic	Pye et al. (2013)
25% of NO_x reduction will reduce 9% bSOA for June 2013 SOAS conditions at Centreville, Alabama.	Positive	CMAQ5.1 with SAPRC07tic (Centreville, AL)	SOA formation based onsemivolatile organic nitrates	Pye et al. (2015)
NO_x and preexisting OA and anthropogenic VOCs enhanced bSOA formation and accounted for 78% of bSOA.	Positive	WRF-CHEM MOZART-MOSAIC (East Asia)	VBS fit to β-pinene + NO_3 experiment	Matsui et al. (2014)
By including aerosol from NO_x-depending nitrate radical oxidation, Terpene (monoterpene + sesquiterpene) aerosol approximately doubles and isoprene aerosol is enhanced by 30 to 40% in the southeastern United States.	Positive	GEOS-CHEM with VBS fit (southeastern United States)	VBS fit with isoprene + NO_3 and terpene NO_3	Pye et al. (2010)
SOA concentrations increase in northern U.S. cities by around 3% but decrease in the rural southeastern United States by approximately 5% with 25% NO_x reduction; 50% reduction in NO_x will decease bSOA by ~0.5 $\mu g/m^3$.	Conditionally Positive	PMCAMx (eastern United States)	NO_3 SOA yields same as photooxidation ($OH + O_3$) yields	Lane et al. (2008)
50% NOx reduction gives limited SOA reductions of 0.9–5.6, 6.4–12.0, and 0.9–2.8% for global, southeastern United States, and Amazon (respectively).	Positive but limited	CAM4 with VBS (Global)	NO_3 SOA yields same as photooxidation (OH + ozone) yields	Zheng et al. (2015)
Measured effect	Effect of NO_x on bSOA	Campaign	Measured correlation	Reference
NO_x positively correlated with nighttime oxidation of bVOCs when NO_x to bVOC ratio is lower than 0.5; they are independent when the ratio is higher than 0.5.	Conditionally Positive	Night-time flights during SENEX	VOCs loss and NO_x	Edwards et al. (2017)
43% to 70% of bSOA are enhanced by NO_x and SO_2.	Positive	SOAS at Centreville, AL	AMS factor LOOA and NO_x	Xu et al. (2015)
NO_x related OM was negatively correlated with bVOCs; NO_x + bVOCs products are more volatile than NO_x + anthropogenic VOC products.	Conditionally Negative	CalNex at Bakersfield, CA	Particulate total alkyl and multifunctional nitrates and NO_x	Rollins et al. (2012)
NO_y suppress bSOA formation through IEPOX pathway.	Negative	Amazon, Brazil	IEPOX SOA and NO_y	De Sa et al. (2017)
High concentrations of NO_x (average: 21 ppb) suppress bSOA formation through IEPOX pathway.	Negative	Nanjing, Eastern China	IEPOX SOA and NO_x	Zhang et al. (2017)
Isoprene SOA yields increase and then decrease as NO_x concentration increases.	Positive and negative	Lab studies	Isoprene SOA yield and NO_x	Kroll et al. (2006; Ng et al. (2007; Xu et al. (2014)
Addition of NO_x has minor effect on SOA yield up to a threshold and SOA yields decrease afterwards.	None or negative	Lab study	Isoprene SOA yield and NO_x	Liu et al. (2016)
Nucleation of bSOA was suppressed by NO_x reactions with monoterpenes.	Negative	Lab study	New particle formation rates and NO_x	Wildt et al. (2014)

changing oxidation pathways and ultimate products (Atkinson et al., 2004; Hoyle et al., 2011; Kroll et al., 2006; Presto et al., 2005; Shrivastava et al., 2017; Surratt et al., 2006; Ziemann & Atkinson, 2012), it is important to quantify them in atmospheric field studies.

Chemical transport models capture some aspects of the influence of NO_x on organic aerosols. Zheng et al. (2015) used an updated SOA scheme in the global NCAR (National Center for Atmospheric Research) Community Atmospheric Model version 4 with chemistry (CAM4-chem) with a four-product volatility basis set scheme with NO_x-dependent SOA yields and aging parameterizations and predicted only 6–12% biogenic SOA decreases in the southeastern United States for 50% NO_x reductions. Pye et al. (2015) updated the comprehensive coupled gas and aerosol processes in CMAQ5.1 with SAPRC07tic (State Air Pollution Research Center mechanism update, https://www.airqualitymodeling.org/index.php/CMAQ_v5.1_SAPRC07tic_AE6i; Hutzell et al., 2012; Lin et al., 2013; Xie et al., 2013). NO_3-related reactions of monoterpenes (MTNO3) and isoprene as well as monoterpene peroxy radical reactions with NO resulted in semivolatile organic nitrates that contributed to organic aerosol (Pye et al., 2015). The model predicted a 25% reduction in NO_x emissions would cause a 9% reduction in organic aerosol for June 2013 in Centreville, Alabama.

These model schemes incorporate the results of laboratory experiments that show that NO_x affects biogenic SOA formation in at least three different, competing, and counteracting ways. First, NO_x can reduce O_3 formation in the high-NO_x regime but under low-NO_x conditions increasing NO_x will result in increases in OH radicals and O_3 (Seinfeld & Pandis, 2016), both of which result in higher SOA yields (Zheng et al., 2015). Second, high concentrations of nighttime nitrate radical (NO_3) increased SOA formation from isoprene in chamber experiments (Ng et al., 2008) by forming organonitrates (Ng et al., 2017). Third, reaction of NO with organo-peroxy radicals (RO_2) in the high NO_x regime can lower SOA yields due to more volatile products compared to reaction with hydroperoxy radicals (HO_2; Kroll et al., 2006; Kroll & Seinfeld, 2008; Zheng et al., 2015; Ziemann & Atkinson, 2012). However, the role of NO_x in systems that undergo autoxidation, particularly monoterpenes (Ehn et al., 2014), has not been elucidated. These multifaceted effects mean that the role of NO_x on biogenic SOA formation in the atmosphere depends on the specific atmospheric conditions and precursors that are present.

In order to use field measurements as constraints for models, we need sufficient aerosol chemical composition measurements to separate biogenic SOA from other organic aerosol components. The separation is difficult because biogenic SOA formation is influenced by the same oxidants that form other SOA, and there is often overlap between primary and secondary emission sources. Positive Matrix Factorization (PMF) of aerosol mass spectrometer (AMS) measurements (Lanz et al., 2007; Ulbrich et al., 2009) use high time resolution to separate small differences in the timing of emissions and photochemical accumulation (Corrigan et al., 2013; Liu et al., 2012), but Fourier transform infrared spectroscopy (FTIR; Hallquist et al., 2009; Russell, 2014; Russell et al., 2009) provides specific chemical fingerprints that associate coemitted primary and secondary components (Russell et al., 2011). For example, PMF of FTIR has provided substantial evidence for nonacid carbonyl groups associated with biogenic SOA in forest conditions (Corrigan et al., 2013; Schwartz et al., 2010; Takahama et al., 2011). One challenge is that a common AMS PMF factor has highly oxidized organic fragments with high *m/z* 28 and *m/z* 44 and accounts for a substantial fraction of OM both from anthropogenic sources like vehicle emissions (Presto et al., 2014) and from natural biogenic emissions (Chen et al., 2015; Xu et al., 2015). In addition, oxidized organic fragments can also result from vegetative detritus (Corrigan et al., 2013; Takahama et al., 2011), which often coincide with biogenic volatile organic compound (bVOC) emissions and contain high O/C from hydroxyl groups in primary plant materials (Medeiros et al., 2006). Biomass burning factors (Corrigan et al., 2013; Hawkins & Russell, 2010; Takahama et al., 2011) from FTIR PMF also have high nonacid carbonyl group content similar to biogenic factors, possibly from oxidation at higher temperatures in wildfires or lower temperatures in residential burning (Corrigan et al., 2013).

FTIR biogenic SOA has been characterized by PMF and clustering in several field studies and shows 15 to 25% hydroxyl, 14 to 41% carbonyl, and 14 to 25% carboxylic acid groups in a variety of atmospheric conditions (Corrigan et al., 2013; Schwartz et al., 2010; Takahama et al., 2011) and chamber studies (Palen et al., 1992; Russell et al., 2011; Schwartz et al., 2010). Organic functional groups of FTIR biogenic factors identified at Whistler, British Colombia, were similar to SOA reported from chamber oxidation of bVOCs (Schwartz et al., 2010).

To understand the influence of NO_x and other pollutants on biogenic SOA, we compared measurements from the Southern Oxidant and Aerosol Study (SOAS) 2013 at Look Rock (LRK), Tennessee, and Centreville (CTR), Alabama. The differences and similarities between the aerosol sources and composition at these two sites were evaluated by comparing the AMS and FTIR PMF factor concentrations with anthropogenic source marker concentrations. Comparisons to FTIR results from lab-generated biogenic SOA properties provide the likely source of biogenic SOA. Model simulations were compared at the two sites and used to investigate the regional representativeness of these two sites. Both the measurements and the simulations illustrate how NO_x affects biogenic SOA composition and concentration in the southeastern United States.

2. Aerosol Measurements at LRK and CTR

Aerosol measurements were made from 1 June 2013 to 18 July 2013 at LRK and CTR in the southeastern United States. The LRK site (35.63314°N, 83.94185°W) is on the northern slope of the Great Smoky Mountains and has an elevation of 801 m above sea level, where a permanent structure with a long-term IMPROVE sampling program has measured O_3 and particulate matter (PM) 2.5 components. The CTR site (32.90289°N, 87.24968°W) is part of the Southeastern Aerosol Research and Characterization (SEARCH) air

quality sampling network within a high isoprene-emitting broadleaf forest and is located on the west side of the Cahaba River at an elevation of 126 m. Both sites are forested and rural. Local times are used in all comparisons to better reflect diurnal patterns in the measurements. Note that in summer LRK uses Eastern Daylight Time zone and CTR uses Central Daylight Time, but time correlations are calculated based on local time at both sites. For example, 4 p.m. EDT at LRK is compared with 4 p.m. CDT at CTR. VOCs are measured at CTR by gas-chromatography mass-spectrometry (GC-MS) as described by Xu et al. (2015). Following Devore and Berk (2012), the Pearson correlation coefficient (r) is used to discriminate among relationships which exhibit weak ($|r| < 0.5$), moderate ($0.5 < |r| < 0.8$), and strong ($|r| > 0.8$) correlations. The $|r| < 0.35$ is identified as "no correlation" (Taylor, 1990).

2.1. Aerosol Particle Measurements

At LRK, a climate-controlled van with an isokinetic inlet pulled air into the van for distribution to a high-resolution time-of-flight AMS, a scanning electrical mobility spectrometer (SEMS), and filters for FTIR and X-ray fluorescence (XRF). At CTR, submicron aerosol particles were collected in a van with air drawn from a window-mounted inlet and through a silica gel denuder with a sharp-cut cyclone for collection of dry PM_1 and $PM_{2.5}$ particles on filters.

Filter samples were collected on prescanned Teflon filters (Teflon, Pall Life Science Inc., 37-mm diameter, 1.0-μm pore size) at CTR and LRK behind PM_1 and $PM_{2.5}$ sharp-cut cyclones (SCC2.229 PM_1 and SCC2.229 $PM_{2.5}$, BGI Inc). Four PM_1 (from 0800 to 1200, from 1200 to 1600, from 1600 to 1900, and from 2000 to 0700 local time) and two $PM_{2.5}$ (from 0800 to 1900 and from 2000 to 0700 local time) samples were collected each day at each site. Samples were frozen and transported to the Scripps laboratory for FTIR spectroscopy. A Bruker Tensor 27 FTIR spectrometer with a deuterated triglycine sulfate detector (Bruker, Waltham, MA) was used to scan the filters both before and after sampling. Filters were installed in the sampling van each morning, and solenoid valves controlled the start and stop of collection; the filter holders were mounted in a 5-ft^3 (0.141584-m^3) refrigerator to keep the filter holders at 4 °C during and after collection each day and minimize losses due to vaporization of higher vapor pressure components, as well as reactions that could change organic composition during storage. An automated algorithm was applied to quantify the mass of the organic functional groups (Russell et al., 2009; Takahama et al., 2013). Five groups (alkane, amine, hydroxyl, carbonyl, and carboxylic acid) were quantified by the area of absorption peaks, and the sum of the mass of the five functional groups is used as the quantified OM (Maria et al., 2002). Absorption peaks for other groups (organosulfate, organonitrate, aromatic, and alkene groups) were fit, but more than 90% of the samples were below the limit of quantification and are excluded. Fifty-four filters at LRK and 2 at CTR were selected for XRF (Chester Labnet, OR) quantification of major elements above 23 amu. The mass of dust was calculated from the XRF metals as described by Usher et al. (2003).

The high-resolution time-of-flight AMS measured nonrefractory particle mass ionized by electron impact after vaporizing at 600–650 °C surface (DeCarlo et al., 2006). The AMS operation, calibration, and measurements at LRK and CTR are reported by Liu et al. (2017) and Xu et al. (2015). Measurements at both sites were collected in two modes: V mode with higher m/z resolving power and W mode with higher mass sensitivity; single-particle light-scattering mode was also used at LRK (Liu et al., 2017; Xu et al., 2015). V mode is reported here because of its high signal sensitivity at 5-min time resolution. Aerosol Chemical Speciation Monitor (ACSM; Ng et al., 2011) was also deployed at LRK, and the ACSM scanning rate was set at 200 ms/amu and collected for 30-min intervals (Budisulistiorini et al., 2015). CE (collection efficiency) was applied to mass concentration from AMS and ACSM. Budisulistiorini et al. (2015) used a CE value of 0.5 calculated based on Middlebrook et al. At LRK, the AMS CE of 0.80 was calculated by scaling to SEMS mass distribution (after removing refractory components) using density of 1.5 (calculated from matching the modal peak from AMS to that from SEMS). AMS CE-corrected sulfate was correlated to sulfate from XRF sulfur with $R = 0.74$ and slope of 1.14 (Liu et al., 2017); at CTR, a composition-dependent CE with a mean value of 0.59 was applied based on the sulfate and ammonium composition (Middlebrook et al., 2012; Xu et al., 2015).

Cloud condensation nuclei (CCN) measurements were collected at LRK and CTR. At CTR, the CCN counter was operated in Scanning Flow CCN Analysis mode (Moore & Nenes, 2009), scanning flow rate sinusoidally from 0.2 to 0.9 L/min then back to 0.2 L/min over 2 min to give CCN spectrum between 0.15 and 0.54% supersaturation (Cerully et al., 2015). At LRK size-resolved CCN measurements were conducted at 0.20%, 0.37%, and 0.58% supersaturation.

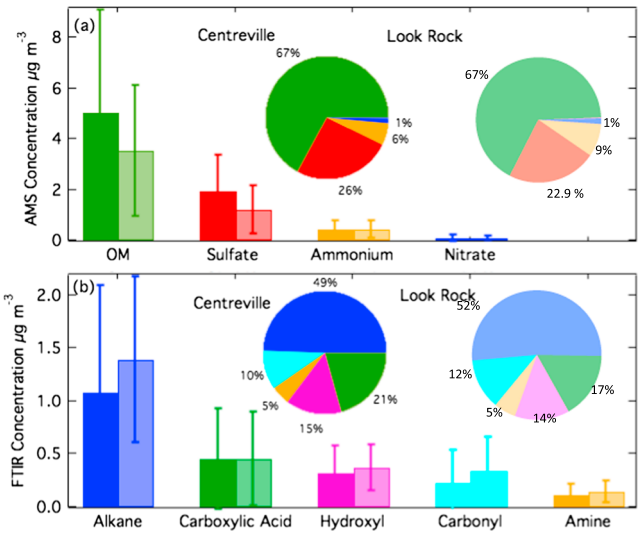

Figure 1. Average of (a) FTIR organic functional group concentrations and (b) AMS OM at LRK and CTR. AMS OM is correlated with FTIR OM (r = 0.75 and 0.65, respectively). The pie charts show the mass fractions of organic functional groups (FTIR) and nonrefractory species (AMS). The bars represent standard deviation of OM concentrations from 1 June 2013 to 18 July 2013.

2.2. CMAQ Model

CMAQ v5.1 simulations described by Pye et al. (2015, 2017) and Murphy et al. (2017) cover the southeastern United States domain for June 2013 at 12 km by 12 km horizontal resolution using meteorology from Advanced Research Weather Research and Forecasting (WRF) model (ARW) version 3.6.1 (Pye et al., 2015, 2017). The model includes gas-phase chemistry based on SAPRC07tic (Xie et al., 2013) with additional updates for the formation of isoprene-epoxydiol (IEPOX) SOA (Pye et al., 2015, 2017) and semivolatile organic nitrates, primarily from monoterpene reactions with nitrate radicals (Pye et al., 2015), as well as other semivolatile SOA (Pye et al., 2017). The semivolatile primary organic aerosol and potential SOA from combustion emissions introduced by Murphy et al. (2017) were included to better represent anthropogenic OM.

2.3. FTIR Measurements of Chamber Experiments

Chamber biogenic SOA experiments were carried out at CU Boulder using isoprene and α-pinene (https://cfpub.epa.gov/ncer_abstracts/index.cfm/fuseaction/display.abstractDetail/abstract/9975/report/F). Three different types of oxidation (NO_3 radicals, O_3, and OH radicals + NO_x) were investigated in the experiments. Neutral ammonium sulfate particles were used as seed particles in some of the experiments. Relative humidity was 50% in all the experiments. NO_3 radicals were formed with N_2O_5 with mixing ratio from 0.33 to 1 ppm. For OH radicals + NO_x conditions, oxidants were 10 ppm CH_3ONO and 10 ppm NO with ultraviolet light. Two FTIR samples were collected on filters in each biogenic SOA formation experiment. The filters were scanned, and spectral peaks were integrated following the same procedure used for the ambient samples (Russell et al., 2009; Takahama et al., 2013).

3. Results

The LRK and CTR sites are influenced by the Bermuda-Azores High in summer, with warm humid air moving northward and northeastward from the Gulf of Mexico into the interior of the continent (Davis et al., 1997). The aerosol particle concentrations accumulated for periods of several days with low wind and little precipitation before being washed out (Liu et al., 2017). The precipitation events overlapped 70% of the time at the two sites during SOAS, synchronizing particle removal and thus contributing to the correlation of the time series of concentrations (Figure S1).

3.1. Fine and Submicron Chemical Components of Aerosols and Level of Pollutants

Figure 1 shows the project average AMS PM_1 nonrefractory component and FTIR functional group mass concentrations. AMS nonrefractory mass had average concentrations of 5.3 ± 3.7 μg/m^3 at LRK and 7.5 ± 4.0 μg/m^3 at CTR. The fractions of nonrefractory components were similar with high OM fractions (67% and 67%, at LRK and CTR, respectively) followed by sulfate (23% and 26% at LRK and CTR, respectively), and ammonium (9% and 6% at LRK and CTR, respectively). Nitrate and chloride mass concentrations were below 2% of OM at both sites (Figure 1). For comparison, ACSM OM concentrations were 4.9 ± 3.0 μg/m^3 at LRK (Budisulistiorini et al., 2015) and 5.2 ± 3.0 μg/m^3 at CTR (Saha et al., 2017). FTIR OM varied from 0.1 to 12 μg/m^3 at LRK and from 0.2 to 12 μg/m^3 at CTR, with average concentrations of 2.7 ± 1.4 μg/m^3 at LRK and 2.7 ± 1.8 μg/m^3 at CTR. The functional group compositions were very similar at the two sites with 52% alkane group mass, followed by 17% carboxylic acid, 14% hydroxyl, 12% carbonyl, and 5% amine group mass at LRK. At CTR, the organic functional group mass fractions were less than 4% different from LRK. $PM_{2.5}$ OM was correlated to that of PM_1 (r = 0.89 and 0.85) but about 15% higher and with similar concentration (2% higher) at LRK and CTR, respectively. $PM_{2.5}$ organic functional group concentrations were also very similar at the two sites.

AMS and FTIR OM concentration had moderate correlation coefficients between the two sites with r = 0.80 at LRK and r = 0.68 at CTR (Figure S2). FTIR OM concentrations were 20% to 40% lower than ACSM and AMS OM at both sites, consistent with the ±20% uncertainty of each measurement, which has been reported in previous studies (Allan, Jimenez, et al., 2003; Allan, Rami Alfarra, et al., 2003; Bahreini et al., 2009; Jimenez

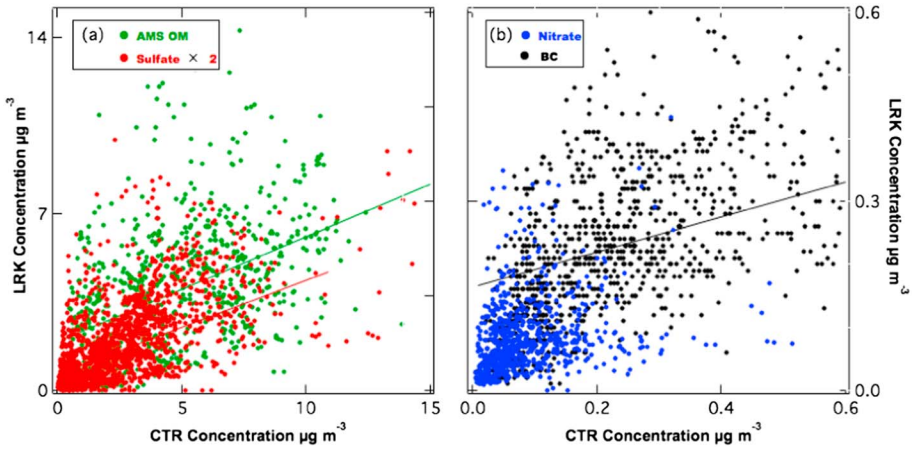

Figure 2. Scatter plots of (a) AMS OM ($\mu g/m^3$) with *r* of 0.47 and slope of 0.37, but plotted with 3 points >15 $\mu g/m^3$ not shown; sulfate ($\mu g/m^3$) with *r* of 0.51 and slope of 0.39, but plotted with 3 points > 15 $\mu g/m^3$ not shown; (b) BC ($\mu g/m^3$) with *r* of 0.40 and slope of 0.27 but plotted with 19 points >0.6 $\mu g/m^3$ not shown; nitrate ($\mu g/m^3$) with *r* of 0.30 and slope of 0.23 at LRK and CTR. (Note that the points not shown in the plots were included in the correlations and slope fits.)

et al., 2016; Russell et al., 2011; Takahama et al., 2013). Much of the AMS uncertainty is associated with correcting ambient measured concentrations by the AMS CE. Since semivolatile compounds may evaporate from filters contributing to lower concentrations, the difference in OM concentration between FTIR and AMS may suggest that there were more semivolatile compounds at CTR, since FTIR has been found to be approximately 70% to 80% of AMS OM at urban sites where substantial hydrocarbon-like organic aerosol has been shown to be semivolatile in other studies (Day et al., 2010; Gilardoni et al., 2009; Liu et al., 2012). Losses of semivolatile components at CTR are also consistent with the CIMS measurements of volatilized OM from a separate set of filters collected at SOAS (Lopez-Hilfiker et al., 2016), which detected 50% of the CTR AMS OM.

OM, sulfate, BC, and CO concentrations as well as particle sizes had weak to moderate correlations (*r* = 0.47, 0.51, 0.40, 0.51, and 0.46, respectively) of the time series at the two sites, and the concentrations were all lower at LRK than CTR (Figures 2 and 3). Average concentrations were 3.6 and 5.0 $\mu g/m^3$ for OM, 1.2 and 1.9 $\mu g/m^3$ for sulfate (both measured by AMS), 0.23 and 0.26 $\mu g/m^3$ for BC, and 115 and 134 ppb for CO at LRK and CTR, respectively. NO_x and NO_y showed almost no correlation of the time series at the two sites, with different mixing ratios and diurnal cycles: NO_x mixing ratio at CTR was 3 to 10 times higher than at LRK during late night and early morning hours (0100–0900) but was roughly the same mixing ratio during the rest of the

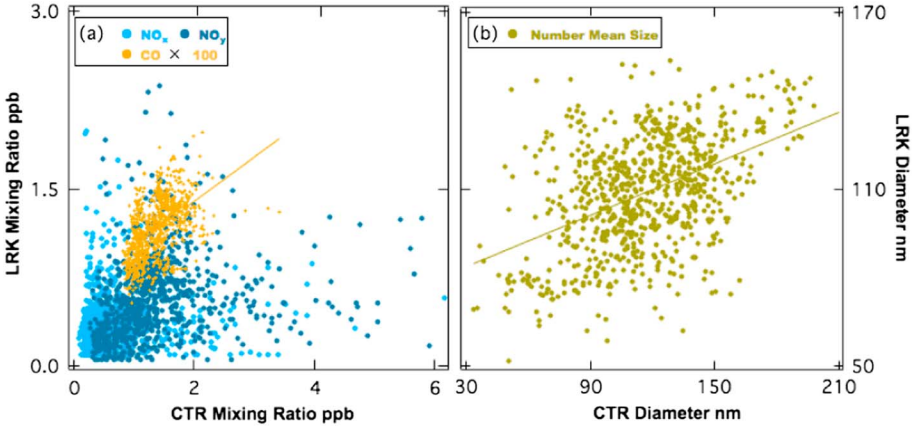

Figure 3. Scatter plots of (a) CO (ppb) with *r* of 0.51 and slope of 0.38; NO_x (ppb) with *r* of 0.08 and slope of 0.03 but with 1 point >6 ppb not shown, and CO and NOx concentrations multiplied by 100; NO_y (ppb) with *r* of 0.22 and slope of 0.10, but with 3 points >6 ppb not shown; (b) SMPS and SEMS number mean size of LRK and CTR. (Note that the points not shown in the plots were included in the correlations and slope fits.)

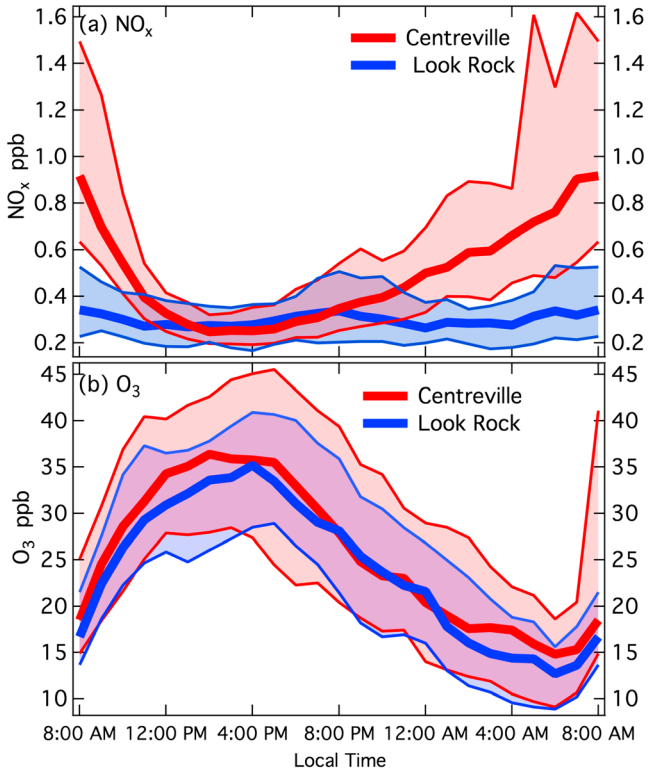

Figure 4. Diurnal plot of (a) NO_x and (b) O_3 at both sites. Medians, 25th percentiles, and 75 percentiles are shown on the figure.

day (Figure 4). The higher mixing ratio at CTR suggests that CTR has more anthropogenic emissions than LRK during SOAS for two reasons: (1) substantial vehicle NO_x emissions surrounding CTR and (2) the higher altitude at LRK (801 m) resulted in less transport of short-lived local emissions. Dust was 3% of submicron mass.

3.2. AMS PMF Organic Factors

The AMS PMF factors that were identified by Xu et al. (2015) and Liu et al. (2017) at LRK and CTR during SOAS include two pairs of factors that showed almost identical *m/z* spectra with cosine similarities higher than 0.98: LRK-Factor44 and CTR-MO-OOA (with characteristic *m/z* 44 signal) and LRK-Factor82 and CTR-Isoprene-OA (with *m/z* 82 signal; Table S1). The factor with high *m/z* 82 was also referred to as 82fac, IEPOX OA, IEPOX-SOA, or Isoprene-OA measured in other studies (Budisulistiorini et al., 2013; Budisulistiorini et al., 2015; Chen et al., 2015; de Sa et al., 2017; Hu et al., 2015; Robinson et al., 2011; Slowik et al., 2011; Xu et al., 2015) as noted in Liu et al. (2017), and showed moderate to strong (r = 0.6 to 0.88) correlations to sulfate: similar to results reported previously (Budisulistiorini et al., 2013, 2015; Xu et al., 2015). The factor with high *m/z* 44 was also referred to as LV-OOA in other publications (Presto et al., 2014; Zhang et al., 2011). Both LRK-Factor44 and CTR-MO-OOA have high contributions of oxygen-containing organic fragments and account for roughly the same fraction of OM (48% at LRK and 39% at CTR). LRK-Factor44 and CTR-MO-OOA have the highest correlation with atmospheric anthropogenic emission tracers (BC, CO, O_3, and NO_y). For example, LRK-Factor44 was correlated to CO (R = 0.61), with O_3 (R = 0.68) and CTR-MO-OOA with CO (R = 0.62), with O_3 (R = 0.49) with 1-hr time resolution. The correlations are more reflective of day-to-day differences. The high *m/z* 44 level suggested that this factor likely includes substantial contributions from secondary sources. LRK-Factor82 and CTR-Isoprene-OA have been associated with isomeric isoprene epoxydiols (IEPOX; Liu et al., 2017; Xu et al., 2015). This factor contributed 20% to OM at LRK and 18% to OM at CTR. CTR had a nighttime factor (CTR-LO-OOA) and a biomass burning factor (CTR-BBOA) but LRK did not. LRK also had a less oxidized daytime OM identified as LRK-Factor91 but no factor similar to CTR-LO-OOA. The LRK AMS PMF factors have cosine similarity greater than 0.6 and temporal correlation coefficient greater than 0.8 for the ACSM PMF factors identified at LRK, which were identified by Budisulistiorini et al. (2015) (Table S1). If the smaller, more common and variable peaks of CO^+, CO_2^+, H_2O^+, and CHO^+ are excluded, the cosine similarity is 0.99 for the *m/z* spectra of CTR-LO-OOA and LRK-Factor91. This indicates that the larger ions at *m/z* 55, 67, 77, and 91, which are more representative of the parent molecules, have consistent relative concentrations that indicate that both factors have contributions from similar bVOCs. Cosine similarity is a measure of angular separation between two nonzero vectors of an inner product space that measures the cosine of the angle between them.

3.3. FTIR PMF Organic Factors

Three factors are identified by PMF from baselined FTIR spectra at both sites by the method of Takahama et al. (2013) as described in the supporting information. More than 85% of the spectra could be reconstructed by the FTIR PMF factors at LRK and more than 87% at CTR. FTIR PMF spectra for PM_1 and $PM_{2.5}$ factors are shown in Figure 5. Spectra of PM_1 and $PM_{2.5}$ factors at both sites are almost identical (cosine similarity $>$ 0.94). Cosine similarities between each of the three identified FTIR factors ranged from 0.40 to 0.75. The first factor contributed 36% and 41% of the FTIR OM at LRK and CTR, respectively, and had high cosine similarity (0.99 at Bakersfield and 0.98 at Hyytiälä) to FTIR spectra of (FFC) factors identified at Bakersfield and Hyytiälä (Corrigan et al., 2013; Liu et al., 2012). Alkane groups made up 70% of the OM of this first factor, followed by hydroxyl (17%) and carboxylic acid (10%) groups. The O/C of the factor is 0.3, indicating a high fraction of hydrocarbon-like organic components. Consequently, the ratio of carboxylic acid and carbonyl groups to alkane groups is the lowest of the three factors, consistent with factors related to combustion emissions in other studies

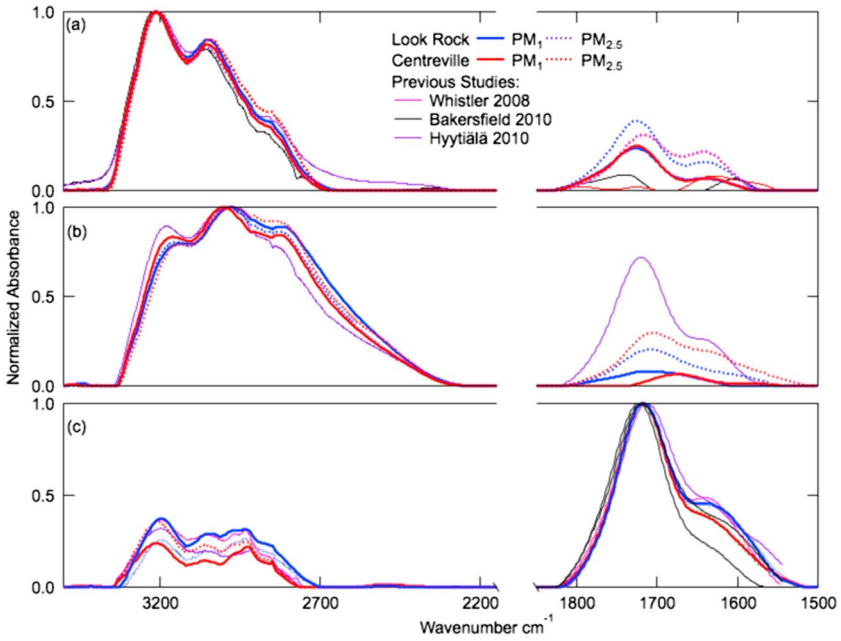

Figure 5. FTR PMF factors spectra in this study as well as Whistler 2008 (Schwartz et al., 2010), Bakersfield 2010 (Liu et al., 2012), and Hyytiälä 2010 (Corrigan et al., 2013): (a) Factors similar to FFC, with cosine similarity higher than 0.97. (b) Factors similar to MOA, with cosine similarity higher than 0.95. (c) Factors similar to BOA, with cosine similarity higher than 0.94.

(Russell et al., 2011). The O/C of 0.3 is similar to values reported for AMS SV-OOA (O/C = 0.37) and higher than those of AMS hydrocarbon-like organic aerosol (O/C = 0.06; Zhang et al., 2011) likely suggesting that the factor includes secondary organic products from combustion sources rather than primary emissions. The factor had weak to moderate correlations with CO (r = 0.53), NO_y (r = 0.40), and BC (r = 0.51) at LRK but had lower correlations with CO (r = 0.28), NO_y (r = 0.23), and BC (r = 0.23) at CTR (Table S2). The FFC factor time series was correlated more strongly to Ca, Mn, and Fe concentrations (r = 0.3 to 0.6) than the other FTIR factors (r = −0.4 to 0.3) at both sites. These metals were found in combustion sources and have served as combustion tracers in previous studies (Agarwal et al., 2015; Cheung et al., 2010; Verma et al., 2010). The FFC factors at the two sites peaked in the late afternoon (1600–1900, 40% higher than the rest of the day), indicating a photochemical contribution to the OM as seen from 8 to 9 June at both sites (Figure S3). This factor has accounted for ~40% of OM at these two rural sites, but it is likely not exclusively from FFC sources. A similar factor accounted for less than 10% of OM at a boreal forest site, consistent with the lower man-made emissions at Whistler (Takahama et al., 2011). This factor is named as FFC factor following the nomenclature of previous studies (Corrigan et al., 2013; Takahama et al., 2011). Although this FFC factor is affected by combustion sources, the weak to intermediate correlations indicate that combustion is not the exclusive source of this factor.

The second factor has substantial alkane group (57%) and also an absorption region at 2,600/cm associated with carboxylic acid groups (23%), making it more oxidized than the FFC factor with an O/C of 0.5. This factor contributed 25% and 27% of FTIR OM at LRK and CTR, respectively. A similar factor was identified in boreal forests in Hyytiälä, Finland (Corrigan et al., 2013), which had a similar spectrum (cosine similarity >0.94, shown in Figure 5) and the highest correlations to sulfate (r = 0.64 and 0.38 for LRK and CTR, respectively), CTR-Isoprene-OA (r = 0.75), and LRK-Factor82 (r = 0.47). This factor had evidence of man-made primary or secondary organic components and is named mixed organic aerosol (MOA) since it has both anthropogenic sulfate and biogenic isoprene-related organic contributions.

The third factor has high carbonyl group absorption at 1,800/cm and contributed 25% OM at LRK and 19% OM at CTR. The high nonacid carbonyl group concentration could indicate that the particles are from both biomass burning and biogenic emissions (as reported previously; Corrigan et al., 2013; Hawkins & Russell, 2010**)**. This factor is identified as biogenic organic aerosols (BOAs) because it includes primary and secondary sources of particles from plant vapor emissions and decaying plant matter. The BOA factor is similar to factors

identified at forested sites (Corrigan et al., 2013; Schwartz et al., 2010), as shown by the similarity of the FTIR spectra in Figure 5, even though monoterpenes may account for more of the bVOC than isoprene at these pine forest sites. The coincidence of the emission timing and locations as well as the similarities in organic functional group biogenic SOA composition does not allow separation of isoprene and monoterpene sources. The largest organic functional group fraction is carbonyl groups (29%), which is consistent with the carbonyl group mass fraction reported for pine forest sites (Corrigan et al., 2013; Schwartz et al., 2010; Takahama et al., 2011). A biomass burning factor (Corrigan et al., 2013; Hawkins & Russell, 2010; Takahama et al., 2011) was not identified by the multihour FTIR samples at either CTR or LRK during SOAS, which is consistent with the small and short-duration biomass burning emissions identified by AMS (Xu et al., 2015). The small methylene peaks in BOA at both CTR and LRK indicate that a very small fraction of BOA could be vegetative detritus. Alkane and hydroxyl groups each contributed approximately 25% of BOA OM. Carboxylic acid and amine group contributions to the BOA factor are lower than 10%, and the factor is highly oxidized with O/C of 0.45. The BOA factor time series correlated to methyl vinyl ketone/methacrolein (MVK/MACR) concentration time series with r = 0.66 at LRK, consistent with these intermediate products serving as markers of isoprene (Liu et al., 2013) and pinene (Zhang et al., 2009) biogenic SOA formation. The correlation of BOA with sulfate is weak with correlation coefficient of 0.45 at LRK and 0.28 at CTR (Table S2), perhaps because the BOA factor does not include the sulfate-enhanced biogenic oxidation products as these may be included in MOA instead.

In summary, FTIR PMF factors were consistent with AMS factors in how OM was apportioned to sources, despite the differences in apportioning oxidized SOA fragments and groups noted by previous work (Corrigan et al., 2013). Specifically, the lower time resolution and lack of fragmentation of FTIR tends to associate oxidation products with functional groups that are associated with products from specific classes of precursor molecules, so that primary and secondary components are in the same factor (Russell et al., 2011). The higher time resolution of AMS often separates primary organic aerosol hydrocarbon fragments that peak in the morning and evening from the SOA fragments produced during afternoon photochemistry. In addition, fragmentation of molecules in the AMS means that many secondary components (such as CO_2^+) occur in different peaks than the primary molecules that may have similar chemical composition that were emitted from the same source. These differences in resolution and fragmentation mean that primary and secondary components from the same source are separated into different factors in AMS measurements even though FTIR tends to retain products from the same source in a single factor. In addition, the higher time resolution AMS chemical signatures identified CTR-BBOA, which only had several 1- or 2-hr sharp concentration peaks during the campaign (Xu et al., 2015).

4. Discussion

The parallel deployment of both FTIR and AMS OM measurement techniques at CTR and LRK during SOAS provided an opportunity to evaluate the similarities and differences of biogenic SOA formation at the different NO_x conditions at the two sites. The chemical compositions of biogenic SOA are very similar at both sites and are similar to chamber experiments, but the minor differences show an important role for NO_x.

4.1. Regional Uniformity of Biogenic SOA in the Southeastern United States

Although the two SOAS sites in this study are approximately 500 km apart, OM, BC, CO, and sulfate concentrations as well as particle size showed weak to moderate correlations of the time series at the two sites (Figures 2 and 3). Organic functional groups and submicron nonrefractory mass components (nitrate, sulfate, organic, and ammonium) were similar fractions of submicron particle mass (Figure 1). OM was approximately 70% and sulfate was 20% of the nonrefractory mass. Oxidized organic functional groups (nonacid carbonyl, hydroxyl, and carboxylic acid) accounted for 50% of OM (Figure 1). Despite the similarity in chemical composition and in submicron particle size (Figures 2, 3, and S4), it is not surprising that the CCN/CN had weak positive correlation at both sites at three different supersaturation levels (r = 0.22 to 0.37; Figure S5). The fact that the correlation is lower relative to the correlations to sulfate, size and number could suggest a role for local factors in organic composition and associated particle hygroscopicity, even though the concentrations are controlled to a substantial extent by scavenging of regional rain (Figure S1). BC and CO are largely driven by precipitation events and regional transport that result in multiday events that overwhelm the local diurnal cycles (Figure S6). These similarities indicate that the aerosol particle concentrations at these two rural

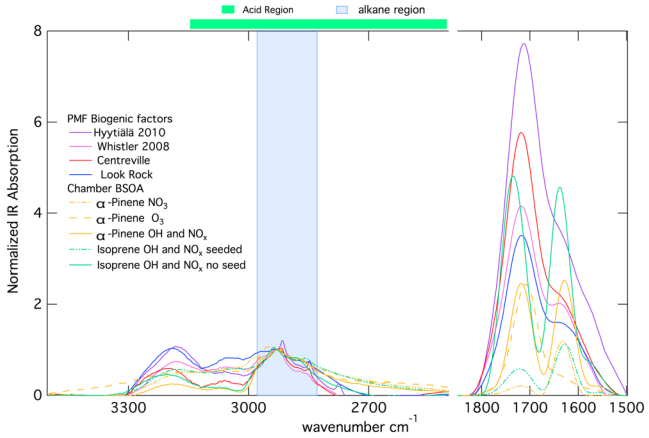

Figure 6. Comparison of laboratory-generated biogenic SOA from α-pinene and isoprene to BOA factors from the SOAS CTR and LRK sites, Whistler (Schwartz et al., 2010), and Hyytiälä (Corrigan et al., 2013). Spectra are normalized at 2,927/cm, a common methylene peak that showed up in all spectra. Ammonium absorption was fitted and removed.

locations in the southeastern United States are controlled both by scavenging of regional rain and by very similar mixtures of precursor emissions and photochemical reaction pathways.

The three very similar FTIR factors and two nearly identical AMS factors measured at both sites were consistent with biogenic SOA formation from largely the same emissions and reactions. The two isoprene-related factors LRK-Factor82 and CTR-Isoprene-OA accounted for approximately 20% of OM and were correlated strongly to sulfate ($r > 0.75$), suggesting that heterogeneous sulfate reactions with IEPOX (Liu et al., 2017) were important at both sites. Factors similar to LRK-Factor82 and CTR-Isoprene-OA were also identified by other summertime studies in the southeastern United States (Budisulistiorini et al., 2016; Budisulistiorini et al., 2017; Xu et al., 2015). LRK-MOA and CTR-MOA from FTIR contributed approximately 25% of OM at each site and had a weak correlation of CTR-MOA to CTR-Isoprene-OA (r = 0.47) and a moderate correlation of LRK-MOA to LRK-Factor91 (r = 0.58), indicating that MOA may also have contributions from biogenic emissions (Budisulistiorini et al., 2015; Xu et al., 2015).

With NO_x + OH and O_3 as oxidants, chamber biogenic SOA were very similar to BOA factors at multiple sites (cosine similarities = 0.84 to 0.90), as shown in Table S3. Most of these chamber and factor spectra (Figure 6) have both acid and nonacid carbonyl groups and similar shapes of peaks, indicating similar mixtures of functional groups. The peak at 3,200/cm shows a high and broad hydroxyl functional group absorption consistent with previous biogenic factors at Whistler (Schwartz et al., 2010). The ammonium peak reflects seed particles in chamber samples, and ambient ammonium peaks in the field samples were removed from spectra. In contrast, low carbonyl and high organonitrate groups measured in the NO_3 oxidation products of α-pinene were not similar to BOA factors (cosine similarities = 0.38 to 0.61). The high degree of similarity of the chamber isoprene and monoterpene biogenic SOA spectra from NO_x + OH and O_3 may be one reason that the FTIR PMF BOA factors from Whistler, Hyytiala, and the southeastern United States are similar even though they have differing amounts of these two bVOCs (Figure 6). The samples from chamber experiments had lower carbonyl group mass concentration compared to the field studies in which biogenic SOA underwent a longer reaction time with lower oxidants compared to chamber. Chamber biogenic SOA had significantly higher organonitrate group fraction (10 to 20% OM) than the ambient BOA, likely because chamber experiments with OH were run in a high NO_x regime, whereas field samples could have had contributions from low NO_x conditions as well. The high oxidant level also contributes to the differences between ambient and chamber biogenic SOA. The seeded chamber biogenic SOA was less similar, possibly because the neutral ammonium sulfate did not represent ambient seeds well. The ammonium subtraction process might also contribute to the difference. CTR-BOA and LRK-BOA could have had contributions from both NO_x + OH and O_3 reactions. FFC and MOA are not similar to chamber biogenic SOA, with cosine similarities lower than 0.4. IEPOX biogenic SOA was not formed because the chamber experiments did not include conditions for low-NO_x, acid-catalyzed chemistry of isoprene oxidation (Lin et al., 2012; Surratt et al., 2007, 2010).

The CMAQ model simulations (Text S3) also had similar concentrations at the two sites, except for the higher monoterpene-related biogenic SOA at CTR (Figure 7). The model components that tracked biogenic SOA from isoprene (Text S3) had similar and substantial concentrations at both sites (0.70 $\mu g/m^3$ at LRK and 0.61 $\mu g/m^3$ at CTR), consistent with the substantial contribution to OM from LRK-Factor82 and CTR-Isoprene-OA. The spatial distribution of simulated IEPOX products is more uniform than the NO_x in the southeastern United States (Figure 8). The sulfate simulated by the CMAQ model was prevalent across the region during the month of June (Figure 8), and distribution of isoprene and monoterpene emissions shows spatial uniformity across the region because of the high forest coverage over most of the region (Guenther et al., 2012; A Guenther et al., 2006; McRoberts et al., 2005). Consistent with this study, simultaneous ACSM and AMS measurements from multiple field campaigns at multiple sites showed that OA is homogeneous in the greater Atlanta area in summer (Xu et al., 2015).

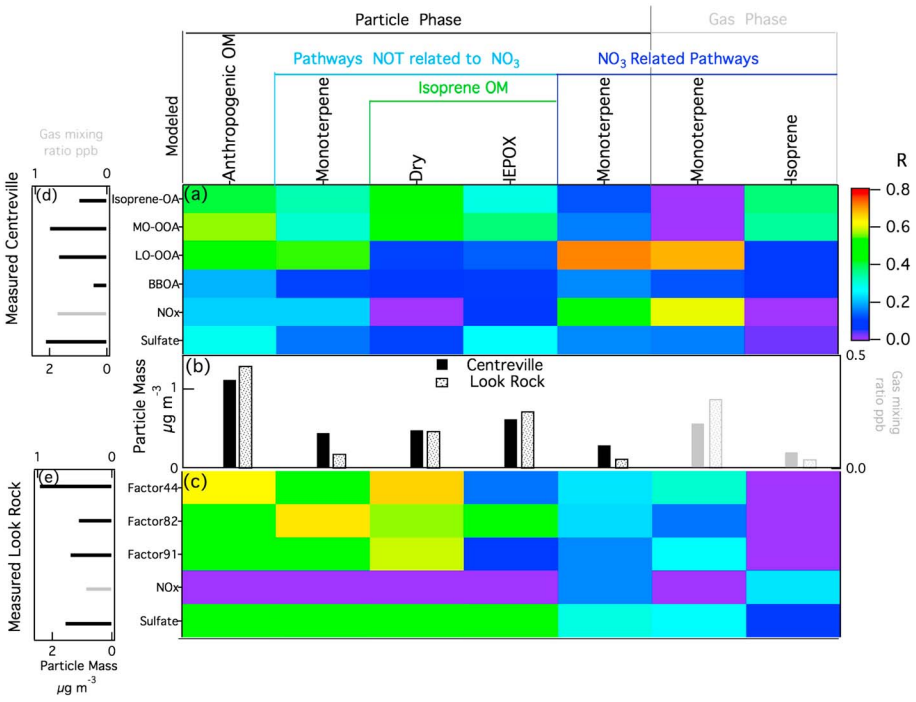

Figure 7. Average concentration of CMAQ modeled species and heat map of correlation coefficients of CMAQ model species to measurements at (a) CTR and (c) LRK. Low 24-hr significance level pairs ($P > 0.05$) are shaded. (b) Concentrations of CMAQ modeled species. Concentrations of measured species at (d) CTR and (e) LRK. Details of the modeled species can be found in Text S3 and Table S7. Low concentration species (<0.05 μg/m^3) are excluded in this figure.

4.2. Differences in NO_x Reactions With bVOC in the Southeastern United States

Despite the regional uniformity of particle composition discussed above, there were also important differences between the two sites. Although the two sites are both rural, LRK is more pristine because it is at 801-m altitude and more than 15 km away from cities and highways, while CTR is at 126-m altitude and also less than 10 km from the Centreville city, resulting in the higher NO_x and NO_y concentrations at CTR than LRK (Figure 3). Aircraft measurements during the campaign showed a consistent NO_x decrease with increasing altitude in the lowest 2 km of the atmosphere, with the NO_x concentration approaching zero at 2 km above ground level (Travis et al., 2016). NO_x concentration at CTR also had a clear peak from 0200 to 0900 (Figure 4). Similar nighttime NO_x increases have been observed at both urban (Alghamdi et al., 2014) and forested sites (Alghamdi et al., 2014; Seok et al., 2013). Limited ventilation of surface NO_x emissions in the low nighttime boundary layers may contribute to this the diurnal pattern. Since the high concentration of NO_x coincides with the northerly wind at CTR (Figure S7), the early morning NO_x peak at CTR is likely due to transport from vehicle sources from the I-20 morning commute, which is located 30 km north of the site. The resulting NO_x spatial distribution (Figure 8) is consistent with National Emissions Inventory at Bibb County (https://www.epa.gov/air-emissions-inventories/national-emissions-inventory-nei), where NO_x is largely from mobile sources (50%)).

Since the measured mixing ratio and diurnal cycle of isoprene (~3 ppb) and monoterpenes (<1 ppb) were similar at the two sites (Budisulistiorini et al., 2015; Xu et al., 2015), the different NO_x loadings at LRK and CTR were likely the cause of the differences in the OM concentrations and diurnal patterns (Liu et al., 2017; Xu et al., 2015). While OM peaked in the early afternoon (1200–2000) at LRK consistently, it peaked both in late afternoon (1800) and at night (0200) at CTR. The nighttime CTR-BOA was 2.5 times higher than the rest of the time, while the nighttime CTR-BOA had similar concentration (92%) with the rest of the time. For example, this diurnal trend is obvious from 11 to 14 June (Figure S3). These different diurnal patterns of the two FTIR BOA factors from LRK and CTR suggest that they were driven by different oxidation pathways. In addition, the correlation of NO_y to O_3 is higher at CTR than LRK in afternoons (1200–1600) with r values of 0.55 and 0.17, respectively, suggesting that NO_x could have contributed to daytime ozone formation at CTR but

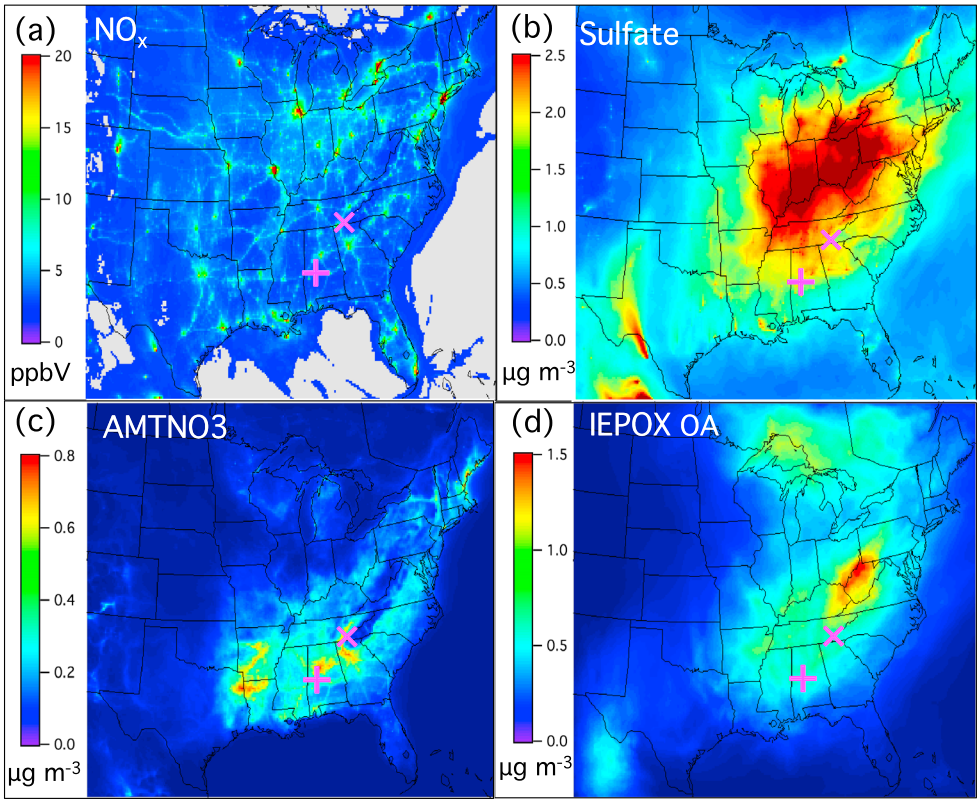

Figure 8. Spatial distribution of (a) NO_x, (b) sulfate, (c) monoterpene organic nitrate biogenic SOA, and (d) IEPOX related biogenic SOA in the southeastern United States from the CMAQ model. The "+" marks Centreville, and the "×" marks Look Rock.

not at LRK (Milford et al., 1994). For this reason, NO_x at CTR may have contributed both directly to biogenic SOA formation and indirectly by increasing O_3.

The direct role of NO_x in contributing to CTR-BOA is evident in its early morning peak similar to that of CTR-LO-OOA (Xu et al., 2015), which suggests a contribution of dark NO_3 oxidation as well as OH + NO_x oxidation (RNO_2 + NO) after sunrise (Lee et al., 2016) that is not present at LRK. Further, the two BOA factors were correlated to NO_x ($r = 0.41$) at CTR but to O_3 ($r = 0.51$) at LRK. NO_x had little correlation to biogenic SOA formation at LRK (Figure S8), and there was no nighttime BOA factor (analogous to CTR-LO-OOA). The daytime LRK-Factor91 accounted for 34% of OM and was correlated to nitrate ($r = 0.65$) and radiation at the surface ($r = 0.83$), consistent with NO_x contributing to oxidants in a photochemically driven reaction. Chamber measurements of *m/z* 91 in products of gas phase isoprene oxidation (Budisulistiorini et al., 2016; Krechmer et al., 2015; Liu et al., 2016; Riva et al., 2017) support this type of formation given the measured *m/z* 91 in LRK-Factor91. Although the factor peaked in daytime with isoprene, we cannot rule out a contribution of monoterpene to this biogenic SOA type (Liu et al., 2017). This factor was not evident at CTR, indicating that its formation may rely on photochemical reactions favored by low NO_x conditions.

CTR-LO-OOA and CTR-BOA had weak to moderate correlations to NO_x ($r = 0.36$ and 0.69, respectively) for NO_x higher than 1 ppb (Figure 9). LRK-Factor91 and LRK-BOA had moderate correlations of the very limited number of measurements for $NO_x > 1$ ppb (Table S4). There was no correlation ($r < 0.2$) of NO_x with CTR-LOOA, LRK-Factor91, CTR-BOA, or LRK-BOA for NO_x mixing ratio below 0.5 ppb (Table S4). The measurements of CTR-LO-OOA and CTR-BOA for NO_x lower than 1 ppb were excluded from the linear regression because the variability below 1 ppb made the correlation coefficients low and fitted slopes uncertain (Table S5). These results suggest that the enhancement of biogenic SOA by NO_x is only clear for NO_x concentrations greater than 1 ppb. NO_x-related enhancement of biogenic SOA formation resulted in 0.5 ± 0.1 $\mu g/m^3$ per 1 ppb NO_x for CTR-LO-OOA and 1.0 ± 0.3 $\mu g/m^{-3}$ per 1 ppb NO_x for CTR-BOA, based on the slopes of the regression lines

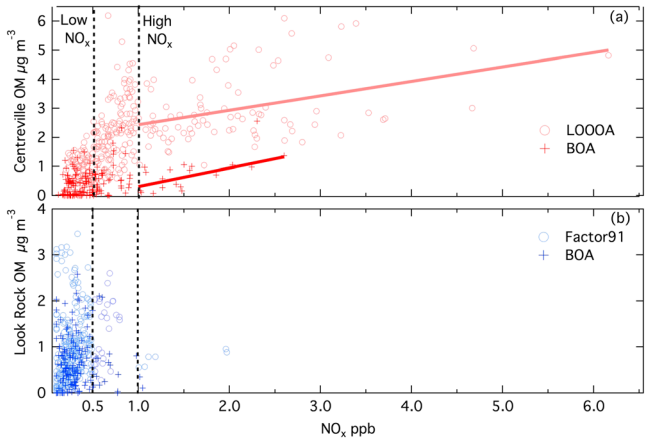

Figure 9. Scatter plot of (a) CTR-LO-OOA, CTR-BOA; (b) LRK-Factor91 and LRK-BOA, and NO_x.

shown. However, it is appropriate to note that the correlations between NO_x and CTR-LO-OOA and CTR-BOA were only weak ($r = 0.36$) and moderate ($r = 0.69$) in the high NO_x regime, which means that even in the high-NOx regime, NO_x explains only 12% to 47% of the variance of the bSOA factors.

The 1 ppb cutoff does not indicate a chemical threshold but rather separates a regime in which the NO_x is sufficiently low that other factors have stronger, or at least comparable, effects on OM concentration. Since these SOAS measurements covered 36 days, variability in wind direction, precipitation, cloudiness, and bVOC emissions also caused day-to-day differences in OM. For example, while the correlation of isoprene to CTR-LO-OOA and CTR-BOA was below $r = 0.3$, monoterpenes were weakly correlated to CTR-LO-OOA when NO_x was lower than 1 ppb ($r \sim 0.4$) but had no correlation ($r = 0.1$) when NO_x was higher than 1 ppb. This moderate correlation of monoterpenes to bSOA at low NO_x is also consistent with monoterpenes being a large source of bSOA at CTR (Zhang et al., 2018). The reason for the difference in correlations to monoterpenes above and below 1 ppb NO_x could be that the monoterpenes are only limiting when NO_x is low. However, given the limited sampling time above 1 ppb NO_x, further measurements would be needed to support this explanation.

In the CMAQ simulation, NO_x and NO_x-related biogenic SOA was more spatially variable than sulfate-related biogenic SOA in the SOAS study region and was very low (<0.2 μg m^{-3}) in some areas, such as at LRK (Figure 7). The high spatial variation of NO_x-related biogenic SOA is consistent with the spatial distribution of NO_x emissions as well as significant contributions from nitrate radical reactions, which tend to occur at night when atmospheric conditions are more stable and reduce transport. Measured NO_x mixing ratio was moderately correlated to model components from NO_3 oxidation products of monoterpene, namely, particle-phase monoterpene-derived organic nitrates (Text S3) at CTR ($r = 0.64$ to 0.72) but not at LRK ($r < 0.25$; Figure 6). The mass concentration of NO_3 oxidation products of monoterpene was 2.3 times higher at CTR at 0.28 μg/m^3 compared to 0.12 μg/m^3 at LRK from the CMAQ model simulation.

5. Conclusions

FTIR and AMS measurements of submicron mass at LRK, Tennessee, and CTR, Alabama, showed that even though CTR had more NO_x from emissions from cities and highways, while LRK was more pristine because of its higher elevation, OM composition and source apportionment were very similar at these two sites, although biomass burning and nighttime NO_x contributed to OM at CTR but not at LRK. The time series of CO, sulfate, BC, and OM concentrations at LRK and CTR had weak and moderate correlations of $r = 0.51$, 0.51, 0.40, and 0.47, respectively. However, NO_x had a very low correlation ($r = 0.08$) between the sites with nighttime-to-early-morning peaks 3 to 10 times higher at CTR than at LRK.

The organic functional group and submicron nonrefractory component (sulfate, nitrate, ammonium, and organic) compositions were very similar at both sites. Three almost identical FTIR PMF factors of both PM_1 and $PM_{2.5}$ had nearly identical contributions to OM with ~40% related to FFC, ~25% related to MOA, and ~20% associated with BOA sources. BOA was similar to chamber SOA generated from both isoprene and monoterpene precursors for NO_x + OH and O_3 oxidants with cosine similarity higher than 0.8. LRK Factor82 and CTR-Isoprene-OA factor was associated with sulfate and with isoprene oxidation products such as IEPOX. This isoprene-related factor contributed 22% at LRK and 18% at CTR, consistent with summertime observations from several other sites in the southeastern United States (Budisulistiorini et al., 2016, 2017; Xu et al., 2015) and despite the differences in NO_x concentrations.

The enhancement of biogenic SOA by NO_x was only evident for NO_x higher than 1 ppb, which only occurred at CTR during SOAS. NO_x enhanced biogenic SOA formation by 0.5 ± 0.1 μg/m^3 for CTR-LO-OOA and 1.0 ± 0.3 μg/m^3 for CTR-BOA above 1 ppb additional biogenic OM for each 1 ppb increase of NO_x. The negligible contribution of NO_x-enhanced OM at lower than 1 ppb NO_x at LRK provided the most striking difference between the two sites. Organic mass (OM) had a maximum in the afternoon at both sites but

increased again during nighttime only at CTR. The correlation of biogenic SOA species from the CMAQ model simulations also showed NO_x produced more OM at CTR during late-night-early-morning periods than at LRK, which may be associated with nitrate-radical oxidation pathways at high NO_x.

Acknowledgments

We thank Ashley Corrigan, Janin Guzman-Morales, and Katie Kolesar for assistance at the LRK field site and Annmarie Carlton, Joost deGouw, Jose Jimenez, and Allen Goldstein for organizing the SOAS campaign. We thank Eric Edgerton for gas concentration and meteorological measurements at Centreville and the IMPROVE network for ozone concentration at Look Rock. We thank Joost deGouw and Allen Goldstein for sharing bVOC measurements at Centreville. We appreciate the support of Sherri Hunt for this project. This work was supported by U.S. Environmental Protection Agency (EPA) grant RD-83540801. Lu Xu and Nga L. Ng acknowledge National Science Foundation grant 1242258 and U.S. Environmental Protection Agency STAR grant RD-83540301. The U.S. EPA through its Office of Research and Development collaborated in the research described here. It has been subjected to Agency administrative review and approved for publication but may not necessarily reflect official Agency policy. The EPA does not endorse any products or commercial services mentioned in this publication. Timothy Bertram was supported by the Office of Science (Office of Biological and Environmental Research), U.S. Department of Energy (grant DE-SC0006431). LRK AMS and FTIR measurements used in this study are curated at http://doi.org/10.6075/J0P26W1T, and all measurements are also available at the project archive http://esrl.noaa.gov/csd/groups/csd7/measurements/2013senex/Ground/DataDownload. CMAQ model code is available via https://github.com/USEPA/CMAQ.

References

Agarwal, A. K., Gupta, T., Shukla, P. C., & Dhar, A. (2015). Particulate emissions from biodiesel fuelled CI engines. *Energy Conversion and Management*, *94*, 311–330. https://doi.org/10.1016/j.enconman.2014.12.094

Alghamdi, M. A., Khoder, M., Harrison, R. M., Hyvärinen, A. P., Hussein, T., al Jeelani, H., et al. (2014). Temporal variations of O-3 and NO_x in the urban background atmosphere of the coastal city Jeddah, Saudi Arabia. *Atmospheric Environment*, *94*, 205–214. https://doi.org/10.1016/j.atmosenv.2014.03.029

Allan, J. D., Jimenez, J. L., Williams, P. I., Alfarra, M. R., Bower, K. N., Jayne, J. T., et al. (2003). Quantitative sampling using an Aerodyne aerosol mass spectrometer: 1. Techniques of data interpretation and error analysis (vol 108, art no 4090, 2003). *Journal of Geophysical Research*, *108*(D9), 4283. https://doi.org/10.1029/2003jd001607

Allan, J. D., Rami Alfarra, M., Bower, K. N., Williams, P. I., Gallagher, M. W., Jimenez, J. L., et al. (2003). Quantitative sampling using an Aerodyne aerosol mass spectrometer: 2. Measurements of fine particulate chemical composition in two UK cities (vol 108, art no 4091, 2003). *Journal of Geophysical Research*, *108*(D9), 4284. https://doi.org/10.1029/2003jd001608

Atkinson, R., Baulch, D. L., Cox, R. A., Crowley, J. N., Hampson, R. F., Hynes, R. G., et al. (2004). Evaluated kinetic and photochemical data for atmospheric chemistry: Volume I - gas phase reactions of O-x, HO_x, NO_x and SO_x species. *Atmospheric Chemistry and Physics*, *4*, 1461–1738.

Bahreini, R., Ervens, B., Middlebrook, A. M., Warneke, C., de Gouw, J. A., DeCarlo, P. F., et al. (2009). Organic aerosol formation in urban and industrial plumes near Houston and Dallas, Texas. *Journal of Geophysical Research*, *114*, D00F16. https://doi.org/10.1029/2008jd011493

Blanchard, C. L., Hidy, G. M., Shaw, S., Baumann, K., & Edgerton, E. S. (2016). Effects of emission reductions on organic aerosol in the southeastern United States. *Atmospheric Chemistry and Physics*, *16*(1), 215–238. https://doi.org/10.5194/acp-16-215-2016

Budisulistiorini, S. H., Baumann, K., Edgerton, E. S., Bairai, S. T., Mueller, S., Shaw, S. L., et al. (2016). Seasonal characterization of submicron aerosol chemical composition and organic aerosol sources in the southeastern United States: Atlanta, Georgia, and Look Rock, Tennessee. *Atmospheric Chemistry and Physics*, *16*(8), 5171–5189. https://doi.org/10.5194/acp-16-5171-2016

Budisulistiorini, S. H., Canagaratna, M. R., Croteau, P. L., Marth, W. J., Baumann, K., Edgerton, E. S., et al. (2013). Real-time continuous characterization of secondary organic aerosol derived from isoprene epoxydiols in downtown Atalanta, Georgia, using the Aerodyne Aerosol Chemical Speciation Monitor. *Environmental Science & Technology*, *47*(11), 5686–5694. https://doi.org/10.1021/es400023n

Budisulistiorini, S. H., Li, X., Bairai, S. T., Renfro, J., Liu, Y., Liu, Y. J., et al. (2015). Examining the effects of anthropogenic emissions on isoprene-derived secondary organic aerosol formation during the 2013 Southern Oxidant and Aerosol Study (SOAS) at the Look Rock, Tennessee ground site. *Atmospheric Chemistry and Physics*, *15*(15), 8871–8888. https://doi.org/10.5194/acp-15-8871-2015

Budisulistiorini, S. H., Nenes, A., Carlton, A. G., Surratt, J. D., McNeill, V. F., & Pye, H. O. T. (2017). Simulating aqueous-phase isoprene-epoxydiol (IEPOX) secondary organic aerosol production during the 2013 Southern Oxidant and Aerosol Study (SOAS). *Environmental Science & Technology*, *51*(9), 5026–5034. https://doi.org/10.1021/acs.est.6b05750

Carlton, A. G., Pinder, R. W., Bhave, P. V., & Pouliot, G. A. (2010). To what extent can biogenic SOA be controlled? *Environmental Science & Technology*, *44*(9), 3376–3380. https://doi.org/10.1021/es903506b

Cerully, K. M., Bougiatioti, A., Hite, J. R., Guo, H., Xu, L., Ng, N. L., et al. (2015). On the link between hygroscopicity, volatility, and oxidation state of ambient and water-soluble aerosols in the southeastern United States. *Atmospheric Chemistry and Physics*, *15*(15), 8679–8694. https://doi.org/10.5194/acp-15-8679-2015

Chen, Q., Farmer, D. K., Rizzo, L. V., Pauliquevis, T., Kuwata, M., Karl, T. G., et al. (2015). Submicron particle mass concentrations and sources in the Amazonian wet season (AMAZE-08). *Atmospheric Chemistry and Physics*, *15*(7), 3687–3701. https://doi.org/10.5194/acp-15-3687-2015

Cheung, K. L., Ntziachristos, L., Tzamkiozis, T., Schauer, J. J., Samaras, Z., Moore, K. F., & Sioutas, C. (2010). Emissions of particulate trace elements, metals and organic species from gasoline, diesel, and biodiesel passenger vehicles and their relation to oxidative potential. *Aerosol Science and Technology*, *44*(7), 500–513. https://doi.org/10.1080/02786821003758294

Corrigan, A. L., Russell, L. M., Takahama, S., Äijälä, M., Ehn, M., Junninen, H., et al. (2013). Biogenic and biomass burning organic aerosol in a boreal forest at Hyytiala, Finland, during HUMPPA-COPEC 2010. *Atmospheric Chemistry and Physics*, *13*(24), 12,233–12,256. https://doi.org/10.5194/acp-13-12233-2013

Davis, R. E., Hayden, B. P., Gay, D. A., Phillips, W. L., & Jones, G. V. (1997). The North Atlantic subtropical anticyclone. *Journal of Climate*, *10*(4), 728–744. https://doi.org/10.1175/1520-0442(1997)010<0728:tnasa>2.0.co;2

Day, D. A., Liu, S., Russell, L. M., & Ziemann, P. J. (2010). Organonitrate group concentrations in submicron particles with high nitrate and organic fractions in coastal southern California. *Atmospheric Environment*, *44*(16), 1970–1979. https://doi.org/10.1016/j.atmosenv.2010.02.045

de Sa, S. S., et al. (2017). Influence of urban pollution on the production of organic particulate matter from isoprene epoxydiols in central Amazonia. *Atmospheric Chemistry and Physics*, *17*(11), 6611–6629. https://doi.org/10.5194/acp-17-6611-2017

DeCarlo, P. F., Kimmel, J. R., Trimborn, A., Northway, M. J., Jayne, J. T., Aiken, A. C., et al. (2006). Field-deployable, high-resolution, time-of-flight aerosol mass spectrometer. *Analytical Chemistry*, *78*(24), 8281–8289. https://doi.org/10.1021/ac061249n

Devore, J. L., & Berk, K. N. (2012). *Modern mathematical statistics with application*, (Second ed.). New York Dordrecht Heidelberg London: Springer Science+Business Media, LLC, Springer. doi:https://doi.org/10.1007/978-1-4614-0391-3

Edwards, P. M., Aikin, K. C., Dube, W. P., Fry, J. L., Gilman, J. B., de Gouw, J. A., et al. (2017). Transition from high- to low-NO_x control of nighttime oxidation in the southeastern US. *Nature Geoscience*, *10*(7), 490−+, doi:https://doi.org/10.1038/ngeo2976), 490–495.

Ehn, M., Thornton, J. A., Kleist, E., Sipilä, M., Junninen, H., Pullinen, I., et al. (2014). A large source of low-volatility secondary organic aerosol. *Nature*, *506*(7489), 476−+, doi:https://doi.org/10.1038/nature13032), 476–479.

Gilardoni, S., Liu, S., Takahama, S., Russell, L. M., Allan, J. D., Steinbrecher, R., et al. (2009). Characterization of organic ambient aerosol during MIRAGE 2006 on three platforms. *Atmospheric Chemistry and Physics*, *9*(15), 5417–5432.

Guenther, A., Karl, T., Harley, P., Wiedinmyer, C., Palmer, P. I., & Geron, C. (2006). Estimates of global terrestrial isoprene emissions using MEGAN (Model of Emissions of Gases and Aerosols from Nature). *Atmospheric Chemistry and Physics*, *6*, 3181–3210.

Guenther, X., Jiang, C., Heald, L., Sakulyanontvittaya, T., Duhl, T., Emmons, L. K., & Wang, X. (2012). The Model of Emissions of Gases and Aerosols from Nature version 2.1 (MEGAN2.1): an extended and updated framework for modeling biogenic emissions. *Geoscientific Model Development*, *5*(6), 1471–1492. https://doi.org/10.5194/gmd-5-1471-2012

Hallquist, M., Wenger, J. C., Baltensperger, U., Rudich, Y., Simpson, D., Claeys, M., et al. (2009). The formation, properties and impact of secondary organic aerosol: current and emerging issues. *Atmospheric Chemistry and Physics*, *9*(14), 5155–5236. https://doi.org/10.5194/acp-9-5155-2009

Hawkins, L. N., & Russell, L. M. (2010). Oxidation of ketone groups in transported biomass burning aerosol from the 2008 Northern California Lightning Series fires. *Atmospheric Environment*, *44*(34), 4142–4154. https://doi.org/10.1016/j.atmosenv.2010.07.036

Hoyle, C. R., Boy, M., Donahue, N. M., Fry, J. L., Glasius, M., Guenther, A., et al. (2011). A review of the anthropogenic influence on biogenic secondary organic aerosol. *Atmospheric Chemistry and Physics*, *11*(1), 321–343. https://doi.org/10.5194/acp-11-321-2011

Hu, W. W., Campuzano-Jost, P., Palm, B. B., Day, D. A., Ortega, A. M., Hayes, P. L., et al. (2015). Characterization of a real-time tracer for isoprene epoxydiols-derived secondary organic aerosol (IEPOX-SOA) from aerosol mass spectrometer measurements. *Atmospheric Chemistry and Physics*, *15*(20), 11,807–11,833. https://doi.org/10.5194/acp-15-11807-2015

Hutzell, W. T., Luecken, D. J., Appel, K. W., & Carter, W. P. L. (2012). Interpreting predictions from the SAPRC07 mechanism based on regional and continental simulations. *Atmospheric Environment*, *46*, 417–429. https://doi.org/10.1016/j.atmosenv.2011.09.030

Jimenez, J. L., Canagaratna, M. R., Drewnick, F., Allan, J. D., Alfarra, M. R., Middlebrook, A. M., et al. (2016). Comment on "The effects of molecular weight and thermal decomposition on the sensitivity of a thermal desorption aerosol mass spectrometer". *Aerosol Science and Technology*, *50*(9), I–XV. https://doi.org/10.1080/02786826.2016.1205728

Krechmer, J. E., Coggon, M. M., Massoli, P., Nguyen, T. B., Crounse, J. D., Hu, W., et al. (2015). Formation of low volatility organic compounds and Secondary Organic Aerosol from isoprene hydroxyhydroperoxide low-NO oxidation. *Environmental Science & Technology*, *49*(17), 10,330–10,339. https://doi.org/10.1021/acs.est.5b02031

Kroll, J. H., Ng, N. L., Murphy, S. M., Flagan, R. C., & Seinfeld, J. H. (2006). Secondary organic aerosol formation from isoprene photooxidation. *Environmental Science & Technology*, *40*(6), 1869–1877. https://doi.org/10.1021/es0524301

Kroll, J. H., & Seinfeld, J. H. (2008). Chemistry of secondary organic aerosol: Formation and evolution of low-volatility organics in the atmosphere. *Atmospheric Environment*, *42*(16), 3593–3624. https://doi.org/10.1016/j.atmosenv.2008.01.003

Lane, T. E., Donahue, N. M., & Pandis, S. N. (2008). Effect of NO_x on secondary organic aerosol concentrations. *Environmental Science & Technology*, *42*(16), 6022–6027. https://doi.org/10.1021/es703225a

Lanz, V. A., Alfarra, M. R., Baltensperger, U., Buchmann, B., Hueglin, C., & Prevot, A. S. H. (2007). Source apportionment of submicron organic aerosols at an urban site by factor analytical modelling of aerosol mass spectra. *Atmospheric Chemistry and Physics*, *7*(6), 1503–1522.

Lee, B. H., Mohr, C., Lopez-Hilfiker, F. D., Lutz, A., Hallquist, M., Lee, L., et al. (2016). Highly functionalized organic nitrates in the southeast United States: Contribution to secondary organic aerosol and reactive nitrogen budgets. *Proceedings of the National Academy of Sciences of the United States of America*, *113*(6), 1516–1521. https://doi.org/10.1073/pnas.1508108113

Lin, Y. H., Zhang, H., Pye, H. O. T., Zhang, Z., Marth, W. J., Park, S., et al. (2013). Epoxide as a precursor to secondary organic aerosol formation from isoprene photooxidation in the presence of nitrogen oxides. *Proceedings of the National Academy of Sciences of the United States of America*, *110*(17), 6718–6723. https://doi.org/10.1073/pnas.1221150110

Lin, Y. H., Zhang, Z., Docherty, K. S., Zhang, H., Budisulistiorini, S. H., Rubitschun, C. L., et al. (2012). Isoprene epoxydiols as precursors to secondary organic aerosol formation: Acid-catalyzed reactive uptake studies with authentic compounds. *Environmental Science & Technology*, *46*(1), 250–258. https://doi.org/10.1021/es202554c

Liu, J., Russell, L. M., Lee, A. K. Y., McKinney, K. A., Surratt, J. D., & Ziemann, P. J. (2017). Observational evidence for pollution-influenced selective uptake contributing to biogenic secondary organic aerosols in the southeastern US. *Geophysical Research Letters*, *44*, 8056–8064. https://doi.org/10.1002/2017gl074665

Liu, J. M., et al. (2016). Efficient isoprene secondary organic aerosol formation from a non-IEPDX pathway. *Environmental Science & Technology*, *50*(18), 9872–9880. https://doi.org/10.1021/acs.est.6b01872

Liu, S., Ahlm, L., Day, D. A., Russell, L. M., Zhao, Y., Gentner, D. R., et al. (2012). Secondary organic aerosol formation from fossil fuel sources contribute majority of summertime organic mass at Bakersfield. *Journal of Geophysical Research*, *117*, D00V26. https://doi.org/10.1029/2012jd018170

Liu, Y. J., Herdlinger-Blatt, I., McKinney, K. A., & Martin, S. T. (2013). Production of methyl vinyl ketone and methacrolein via the hydroperoxyl pathway of isoprene oxidation. *Atmospheric Chemistry and Physics*, *13*(11), 5715–5730. https://doi.org/10.5194/acp-13-5715-2013

Lopez-Hilfiker, F. D., Mohr, C., D'Ambro, E. L., Lutz, A., Riedel, T. P., Gaston, C. J., et al. (2016). Molecular composition and volatility of organic aerosol in the Southeastern US: implications for IEPDX derived SOA. *Environmental Science & Technology*, *50*(5), 2200–2209. https://doi.org/10.1021/acs.est.5b04769

Maria, S. F., Russell, L. M., Turpin, B. J., & Porcja, R. J. (2002). FTIR measurements of functional groups and organic mass in aerosol samples over the Caribbean. *Atmospheric Environment*, *36*(33), 5185–5196. https://doi.org/10.1016/s1352-2310(02)00654-4

Matsui, H., Koike, M., Kondo, Y., Takami, A., Fast, J. D., Kanaya, Y., & Takigawa, M. (2014). Volatility basis-set approach simulation of organic aerosol formation in East Asia: Implications for anthropogenic-biogenic interaction and controllable amounts. *Atmospheric Chemistry and Physics*, *14*(18), 9513–9535. https://doi.org/10.5194/acp-14-9513-2014

McRoberts, R. E., Bechtold, W. A., Patterson, P. L., Scott, C. T., & Reams, G. A. (2005). The enhanced forest inventory and analysis program of the USDA Forest Service: Historical perspective and announcement of statistical documentation. *Journal of Forestry*, *103*(6), 304–308.

Medeiros, P. M., Conte, M. H., Weber, J. C., & Simoneit, B. R. T. (2006). Sugars as source indicators of biogenic organic carbon in aerosols collected above the Howland Experimental Forest, Maine. *Atmospheric Environment*, *40*(9), 1694–1705. https://doi.org/10.1016/j.atmosenv.2005.11.001

Middlebrook, A. M., Bahreini, R., Jimenez, J. L., & Canagaratna, M. R. (2012). Evaluation of composition-dependent collection efficiencies for the aerodyne aerosol mass spectrometer using field data. *Aerosol Science and Technology*, *46*(3), 258–271. https://doi.org/10.1080/02786826.2011.620041

Milford, J. B., Gao, D. F., Zafirakou, A., & Pierce, T. E. (1994). Ozone precursor levels and responses to emissions reductions analysis of regional oxidant model results. *Atmospheric Environment*, *28*(12), 2093–2104. https://doi.org/10.1016/1352-2310(94)90476-6

Moore, R. H., & Nenes, A. (2009). Scanning flow CCN analysis—A method for fast measurements of CCN Spectra. *Aerosol Science and Technology*, *43*(12), 1192–1207. https://doi.org/10.1080/02786820903289780

Murphy, B. N., Woody, M. C., Jimenez, J. L., Carlton, A. M. G., Hayes, P. L., Liu, S., et al. (2017). Semivolatile POA and parameterized total combustion SOA in CMAQv5. 2: impacts on source strength and partitioning. *Atmospheric Chemistry and Physics*, *17*(18), 11,107–11,133.

Ng, N. L., Brown, S. S., Archibald, A. T., Atlas, E., Cohen, R. C., Crowley, J. N., et al. (2017). Nitrate radicals and biogenic volatile organic compounds: oxidation, mechanisms, and organic aerosol. *Atmospheric Chemistry and Physics*, *17*(3), 2103–2162. https://doi.org/10.5194/acp-17-2103-2017

Ng, N. L., Chhabra, P. S., Chan, A. W. H., Surratt, J. D., Kroll, J. H., Kwan, A. J., et al. (2007). Effect of NOx level on secondary organic aerosol (SOA) formation from the photooxidation of terpenes. *Atmospheric Chemistry and Physics*, *7*(19), 5159–5174. https://doi.org/10.5194/acp-7-5159-2007

Ng, N. L., Herndon, S. C., Trimborn, A., Canagaratna, M. R., Croteau, P. L., Onasch, T. B., et al. (2011). An Aerosol Chemical Speciation Monitor (ACSM) for routine monitoring of the composition and mass concentrations of ambient aerosol. *Aerosol Science and Technology*, *45*(7), 780–794. https://doi.org/10.1080/02786826.2011.560211

Ng, N. L., Kwan, A. J., Surratt, J. D., Chan, A. W. H., Chhabra, P. S., Sorooshian, A., et al. (2008). Secondary organic aerosol (SOA) formation from reaction of isoprene with nitrate radicals (NO3). *Atmospheric Chemistry and Physics*, *8*(14), 4117–4140. https://doi.org/10.5194/acp-8-4117-2008

Palen, E. J., Allen, D. T., Pandis, S. N., Paulson, S. E., Seinfeld, J. H., & Flagan, R. C. (1992). Fourier transform infrared analysis of aerosol formed in the photooxidation of isoprene and beta pinene. *Atmospheric Environment Part a-General Topics*, *26*(7), 1239–1251. https://doi.org/10.1016/0960-1686(92)90385-x

Presto, A. A., Gordon, T. D., & Robinson, A. L. (2014). Primary to secondary organic aerosol: Evolution of organic emissions from mobile combustion sources. *Atmospheric Chemistry and Physics*, *14*(10), 5015–5036. https://doi.org/10.5194/acp-14-5015-2014

Presto, A. A., Hartz, K. E. H., & Donahue, N. M. (2005). Secondary organic aerosol production from terpene ozonolysis. 2. Effect of NO_x concentration. *Environmental Science & Technology*, *39*(18), 7046–7054. https://doi.org/10.1021/es050400s

Pye, H. O. T., Chan, A. W. H., Barkley, M. P., & Seinfeld, J. H. (2010). Global modeling of organic aerosol: The importance of reactive nitrogen (NO_x and NO_3). *Atmospheric Chemistry and Physics*, *10*(22), 11,261–11,276. https://doi.org/10.5194/acp-10-11261-2010

Pye, H. O. T., Luecken, D. J., Xu, L., Boyd, C. M., Ng, N. L., Baker, K. R., et al. (2015). Modeling the current and future roles of particulate organic nitrates in the southeastern United States. *Environmental Science & Technology*, *49*(24), 14,195–14,203. https://doi.org/10.1021/acs.est.5b03738

Pye, H. O. T., Murphy, B. N., Xu, L., Ng, N. L., Carlton, A. G., Guo, H., et al. (2017). On the implications of aerosol liquid water and phase separation for organic aerosol mass. *Atmospheric Chemistry and Physics*, *17*(1), 343–369. https://doi.org/10.5194/acp-17-343-2017

Pye, H. O. T., Pinder, R. W., Piletic, I. R., Xie, Y., Capps, S. L., Lin, Y. H., et al. (2013). Epoxide pathways improve model predictions of isoprene markers and reveal key role of acidity in aerosol formation. *Environmental Science & Technology*, *47*(19), 11,056–11,064. https://doi.org/10.1021/es402106h

Riva, M., Budisulistiorini, S. H., Zhang, Z. F., Gold, A., Thornton, J. A., Turpin, B. J., & Surratt, J. D. (2017). Multiphase reactivity of gaseous hydroperoxide oligomers produced from isoprene ozonolysis in the presence of acidified aerosols. *Atmospheric Environment*, *152*, 314–322. https://doi.org/10.1016/j.atmosenv.2016.12.040

Robinson, N. H., Hamilton, J. F., Allan, J. D., Langford, B., Oram, D. E., Chen, Q., et al. (2011). Evidence for a significant proportion of secondary organic aerosol from isoprene above a maritime tropical forest. *Atmospheric Chemistry and Physics*, *11*(3), 1039–1050. https://doi.org/10.5194/acp-11-1039-2011

Rollins, A. W., Browne, E. C., Min, K. E., Pusede, S. E., Wooldridge, P. J., Gentner, D. R., et al. (2012). Evidence for NOx control over nighttime SOA formation. *Science*, *337*(6099), 1210–1212. https://doi.org/10.1126/science.1221520

Russell, L. M. (2014). Carbonaceous particles: Source-based characterization of their formation, composition, and structures. In K. K. Turekian (Ed.), *Treatise on geochemistry* (Second ed., pp. 291–316). Oxford: Elsevier. doi:https://doi.org/10.1016/B1978–1010–1008-095975-095977.000415-095970

Russell, L. M., Bahadur, R., Hawkins, L. N., Allan, J., Baumgardner, D., Quinn, P. K., & Bates, T. S. (2009). Organic aerosol characterization by complementary measurements of chemical bonds and molecular fragments. *Atmospheric Environment*, *43*(38), 6100–6105. https://doi.org/10.1016/j.atmosenv.2009.09.036

Russell, L. M., Bahadur, R., & Ziemann, P. J. (2011). Identifying organic aerosol sources by comparing functional group composition in chamber and atmospheric particles. *Proceedings of the National Academy of Sciences of the United States of America*, *108*(9), 3516–3521. https://doi.org/10.1073/pnas.1006461108

Saha, P. K., Khlystov, A., Yahya, K., Zhang, Y., Xu, L., Ng, N. L., & Grieshop, A. P. (2017). Quantifying the volatility of organic aerosol in the southeastern US. *Atmospheric Chemistry and Physics*, *17*(1), 501–520. https://doi.org/10.5194/acp-17-501-2017

Schwartz, R. E., Russell, L. M., Sjostedt, S. J., Vlasenko, A., Slowik, J. G., Abbatt, J. P. D., et al. (2010). Biogenic oxidized organic functional groups in aerosol particles from a mountain forest site and their similarities to laboratory chamber products. *Atmospheric Chemistry and Physics*, *10*(11), 5075–5088. https://doi.org/10.5194/acp-10-5075-2010

Seinfeld, J. H., & Pandis, S. N. (2016). *Atmospheric chemistry and physics: From air pollution to climate change* (3rd Edition, 3rd ed., p. 1152). New York, New York, NY: Wiley.

Seok, B., Helmig, D., Ganzeveld, L., Williams, M. W., & Vogel, C. S. (2013). Dynamics of nitrogen oxides and ozone above and within a mixed hardwood forest in northern Michigan. *Atmospheric Chemistry and Physics*, *13*(15), 7301–7320. https://doi.org/10.5194/acp-13-7301-2013

Shilling, J. E., Zaveri, R. A., Fast, J. D., Kleinman, L., Alexander, M. L., Canagaratna, M. R., et al. (2013). Enhanced SOA formation from mixed anthropogenic and biogenic emissions during the CARES campaign. *Atmospheric Chemistry and Physics*, *13*(4), 2091–2113. https://doi.org/10.5194/acp-13-2091-2013

Shrivastava, M., Cappa, C. D., Fan, J., Goldstein, A. H., Guenther, A. B., Jimenez, J. L., et al. (2017). Recent advances in understanding secondary organic aerosol: Implications for global climate forcing. *Reviews of Geophysics*, *55*, 509–559. https://doi.org/10.1002/2016rg000540

Slowik, J. G., Brook, J., Chang, R. Y. W., Evans, G. J., Hayden, K., Jeong, C. H., et al. (2011). Photochemical processing of organic aerosol at nearby continental sites: Contrast between urban plumes and regional aerosol. *Atmospheric Chemistry and Physics*, *11*(6), 2991–3006. https://doi.org/10.5194/acp-11-2991-2011

Spracklen, D. V., Jimenez, J. L., Carslaw, K. S., Worsnop, D. R., Evans, M. J., Mann, G. W., et al. (2011). Aerosol mass spectrometer constraint on the global secondary organic aerosol budget. *Atmospheric Chemistry and Physics*, *11*(23), 12,109–12,136. https://doi.org/10.5194/acp-11-12109-2011

Surratt, J. D., Chan, A. W. H., Eddingsaas, N. C., Chan, M., Loza, C. L., Kwan, A. J., et al. (2010). Reactive intermediates revealed in secondary organic aerosol formation from isoprene. *Proceedings of the National Academy of Sciences of the United States of America*, *107*(15), 6640–6645. https://doi.org/10.1073/pnas.0911114107

Surratt, J. D., Lewandowski, M., Offenberg, J. H., Jaoui, M., Kleindienst, T. E., Edney, E. O., & Seinfeld, J. H. (2007). Effect of acidity on secondary organic aerosol formation from isoprene. *Environmental Science & Technology*, *41*(15), 5363–5369. https://doi.org/10.1021/es0704176

Surratt, J. D., Murphy, S. M., Kroll, J. H., Ng, N. L., Hildebrandt, L., Sorooshian, A., et al. (2006). Chemical composition of secondary organic aerosol formed from the photooxidation of isoprene. *Journal of Physical Chemistry A*, *110*(31), 9665–9690. https://doi.org/10.1021/jp061734m

Takahama, S., Johnson, A., & Russell, L. M. (2013). Quantification of carboxylic and carbonyl functional groups in organic aerosol infrared absorbance spectra. *Aerosol Science and Technology*, *47*(3), 310–325. https://doi.org/10.1080/02786826.2012.752065

Takahama, S., Schwartz, R. E., Russell, L. M., Macdonald, A. M., Sharma, S., & Leaitch, W. R. (2011). Organic functional groups in aerosol particles from burning and non-burning forest emissions at a high-elevation mountain site. *Atmospheric Chemistry and Physics*, *11*(13), 6367–6386. https://doi.org/10.5194/acp-11-6367-2011

Taylor, R. (1990). Interpretation of the correlation-coefficient—A basic review. *Journal of Diagnostic Medical Sonography*, *6*(1), 35–39. https://doi.org/10.1177/875647939000600106

Travis, K. R., Jacob, D. J., Fisher, J. A., Kim, P. S., Marais, E. A., Zhu, L., et al. (2016). Why do models overestimate surface ozone in the Southeast United States? *Atmospheric Chemistry and Physics*, *16*(21), 13,561–13,577. https://doi.org/10.5194/acp-16-13561-2016

Ulbrich, I. M., Canagaratna, M. R., Zhang, Q., Worsnop, D. R., & Jimenez, J. L. (2009). Interpretation of organic components from Positive Matrix Factorization of aerosol mass spectrometric data. *Atmospheric Chemistry and Physics*, *9*(9), 2891–2918.

Usher, C. R., Michel, A. E., & Grassian, V. H. (2003). Reactions on mineral dust. *Chemical Reviews*, *103*(12), 4883–4939. https://doi.org/10.1021/cr020657y

Verma, V., Shafer, M. M., Schauer, J. J., & Sioutas, C. (2010). Contribution of transition metals in the reactive oxygen species activity of PM emissions from retrofitted heavy-duty vehicles. *Atmospheric Environment*, *44*(39), 5165–5173. https://doi.org/10.1016/j.atmosenv.2010.08.052

Wildt, J., Mentel, T. F., Kiendler-Scharr, A., Hoffmann, T., Andres, S., Ehn, M., et al. (2014). Suppression of new particle formation from monoterpene oxidation by NOx. *Atmospheric Chemistry and Physics*, *14*(6), 2789–2804. https://doi.org/10.5194/acp-14-2789-2014

Xie, Y., Paulot, F., Carter, W. P. L., Nolte, C. G., Luecken, D. J., Hutzell, W. T., et al. (2013). Understanding the impact of recent advances in isoprene photooxidation on simulations of regional air quality. *Atmospheric Chemistry and Physics*, *13*(16), 8439–8455. https://doi.org/10.5194/acp-13-8439-2013

Xu, L., Guo, H., Boyd, C. M., Klein, M., Bougiatioti, A., Cerully, K. M., et al. (2015). Effects of anthropogenic emissions on aerosol formation from isoprene and monoterpenes in the southeastern United States. *Proceedings of the National Academy of Sciences of the United States of America*, *112*(1), 37–42. https://doi.org/10.1073/pnas.1417609112

Xu, L., Kollman, M. S., Song, C., Shilling, J. E., & Ng, N. L. (2014). Effects of NO_x on the volatility of secondary organic aerosol from isoprene photooxidation. *Environmental Science & Technology*, *48*(4), 2253–2262. https://doi.org/10.1021/es404842g

Xu, L., Middlebrook, A. M., Liao, J., de Gouw, J. A., Guo, H., Weber, R. J., et al. (2016). Enhanced formation of isoprene-derived organic aerosol in sulfur-rich power plant plumes during Southeast Nexus. *Journal of Geophysical Research-Atmospheres*, *121*, 11,137–11,153. https://doi.org/10.1002/2016jd025156

Xu, L., Suresh, S., Guo, H., Weber, R. J., & Ng, N. L. (2015). Aerosol characterization over the southeastern United States using high-resolution aerosol mass spectrometry: Spatial and seasonal variation of aerosol composition and sources with a focus on organic nitrates. *Atmospheric Chemistry and Physics*, *15*(13), 7307–7336. https://doi.org/10.5194/acp-15-7307-2015

Zhang, H., Yee, L. D., Lee, B. H., Curtis, M. P., Worton, D. R., Isaacman-VanWertz, G., et al. (2018). Monoterpenes are the largest source of summertime organic aerosol in the southeastern United States. *Proceedings of the National Academy of Sciences*, *115*(9), 2038–2043.

Zhang, Q., Jimenez, J. L., Canagaratna, M. R., Ulbrich, I. M., Ng, N. L., Worsnop, D. R., & Sun, Y. L. (2011). Understanding atmospheric organic aerosols via factor analysis of aerosol mass spectrometry: a review. *Analytical and Bioanalytical Chemistry*, *401*(10), 3045–3067. https://doi.org/10.1007/s00216-011-5355-y

Zhang, X., Chen, Z. M., Wang, H. L., He, S. Z., & Huang, D. M. (2009). An important pathway for ozonolysis of alpha-pinene and beta-pinene in aqueous phase and its atmospheric implications. *Atmospheric Environment*, *43*(29), 4465–4471. https://doi.org/10.1016/j.atmosenv.2009.06.028

Zhang, Y. J., et al. (2017). Limited formation of isoprene epoxydiols-derived secondary organic aerosol under NOx-rich environments in Eastern China. *Geophysical Research Letters*, *44*, 2035–2043. https://doi.org/10.1002/2016gl072368

Zheng, Y., Unger, N., Hodzic, A., Emmons, L., Knote, C., Tilmes, S., et al. (2015). Limited effect of anthropogenic nitrogen oxides on secondary organic aerosol formation. *Atmospheric Chemistry and Physics*, *15*(23), 13,487–13,506. https://doi.org/10.5194/acp-15-13487-2015

Ziemann, P. J., & Atkinson, R. (2012). Kinetics, products, and mechanisms of secondary organic aerosol formation. *Chemical Society Reviews*, *41*(19), 6582–6605. https://doi.org/10.1039/c2cs35122f